Controls on the carbon isotopic composition of Southern Ocean phytoplankton

Brian N. Popp,[1] Tom Trull,[2,3] Fabien Kenig,[1] Stuart G. Wakeham,[4] Terri M. Rust,[1] Bronte Tilbrook,[2,5] F. Brian Griffiths,[2,5] Simon W. Wright,[6] Harvey J. Marchant,[6] Robert R. Bidigare,[1] and Edward A. Laws[1]

Abstract. Carbon isotopic compositions of suspended organic matter and biomarker compounds were determined for 59 samples filtered from Southern Ocean surface waters in January 1994 along two north-south transects (WOCE SR3 from Tasmania to Antarctica, and across the Princess Elizabeth Trough (PET) east of Prydz Bay, Antarctica). Along the SR3 line, bulk organic matter show generally decreasing ^{13}C contents southward, which are well correlated with increasing dissolved molecular carbon dioxide concentrations, $CO_2(aq)$. This relationship does not hold along the PET transect. Using concentrations and isotopic compositions of molecular compounds, we evaluate the relative roles of several factors affecting the $\delta^{13}C$ of Southern Ocean suspended particulate organic matter. Along the WOCE SR3 transect, the concentration of $CO_2(aq)$ plays an important role. It is well described by a supply versus demand model for the extent of cellular CO_2 utilization and its associated linear dependence of isotopic fractionation (ε_p) on the reciprocal of $CO_2(aq)$. An equally important factor appears to be changes in algal assemblages along the SR3 transect, with their contribution to isotopic fractionation also well described by the supply and demand model, when formulated to include the cell surface/volume control of supply. Changes in microalgal growth rates appear to have a minor effect on ε_p. Along the PET transect, algal assemblage changes and possibly changes in microalgal growth rates appear to strongly affect the carbon isotopic variations of suspended organic matter. These results can be used to improve the formulation of modern carbon cycle models that include phytoplankton carbon isotopic fractionation.

1. Introduction

The physical circulation of the Southern Ocean contributes dramatically to global climate control by directly linking surface waters with the deep sea in the three major ocean basins and by redistributing waters among them via the Antarctic Circumpolar Current. Biological activity in the Southern Ocean may also be important to global climate. Enhanced primary production rates in the Southern Ocean have been suggested as a means of explaining low-atmospheric CO_2 concentrations during the last glacial period [e.g., *Knox and McElroy*, 1984; *Sarmiento and Toggweiler*, 1984]. Several causal scenarios have been hypothesized and include (1) iron-stimulated increases in export production in the Subantarctic and Polar Frontal Zones of the Southern Ocean [*Martin*, 1990], (2) iron-stimulated increases in export production north of the Antarctic Polar Front (PF) [*Kumar et al.*, 1993], and (3) increased surface water stratification south of

the PF [*François et al.*, 1997]. The two former explanations represent "biological" processes, while the latter is principally a physical phenomenon. Carbon isotopic records of Southern Ocean sedimentary organic matter show clear and dramatic changes from the time of the last glacial maximum to the present and may contain important information about changes in both biological carbon fixation and oceanic circulation during this interval [*Fischer et al.*, 1997] because phytoplankton carbon isotopic compositions appear to reflect a balance of environmental CO_2 supply and biological demand [e.g., *Rau et al.*, 1992; *François et al.*, 1993; *Goericke et al.*, 1994]. Before quantitative constraints can be placed on biological and physical factors from the $\delta^{13}C$ of sedimentary organic materials, fundamental information on the mechanisms controlling the isotopic compositions of phytoplankton and bulk suspended, sinking, and sedimented particulate organic matter in the Southern Ocean is needed.

Stable isotopic characterization of marine organic matter provides important insights into the environmental conditions under which carbon fixation occurs. Early on, *Sackett et al.* [1965; 1974] found that Southern Ocean plankton and sediments have significantly lower $^{13}C/^{12}C$ ratios relative to those at lower latitudes. Subsequent studies of the isotopic composition of marine particulate organic matter at high latitudes [*Wada et al.*, 1987; *Rau et al.*, 1989, 1991a, b; *Bathmann et al.*, 1991; *Fischer*, 1991; *Dunbar and Leventer*, 1992; *Rogers and Dunbar*, 1993; *François et al.*, 1993; *Goericke and Fry*, 1994; *Kennedy and Robertson*, 1995; *Kopczynska et al.*, 1995; *Dehairs et al.*, 1997; *Fischer et al.*, 1997] have confirmed the extreme isotopic nature of Southern Ocean organic matter, which some have related to

[1]School of Ocean and Earth Science and Technology, University of Hawaii, Honolulu.

[2]Antarctic CRC, University of Tasmania, Hobart, Tasmania, Australia.

[3]Now at Department of Geological Sciences, University of Illinois at Chicago.

[4]Skidaway Institute of Oceanography, Savannah, Georgia.

[5]Also at CSIRO, Division of Marine Research, Hobart, Tasmania, Australia.

[6]Australian Antarctic Division, Kingston, Tasmania, Australia.
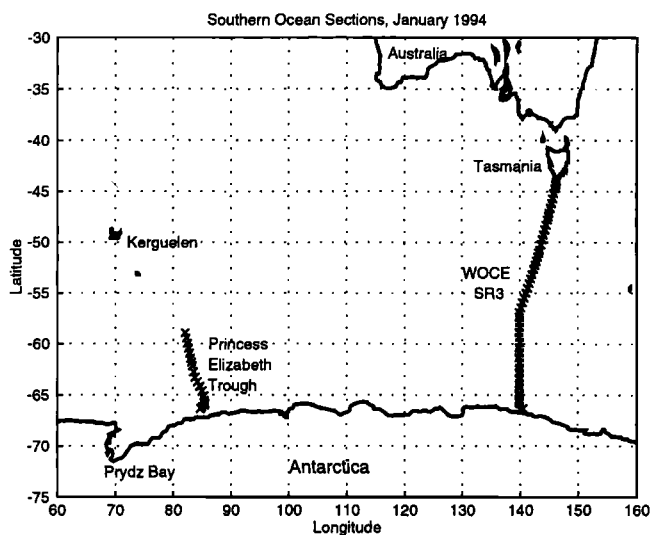
Southern Ocean Sections, January 1994

Figure 1. Map of sample collection sites, along the World Ocean Circulation Experiment (WOCE) SR3 (Hobart to Antarctica, cruise track from 45°55'S, 140°E to 65°24'S, 140°E) and across the Princess Elizabeth Trough (PET), from the West Ice Shelf to the Kerguelen Plateau (58°55'S, 82°01'E to 65°19'S, 84° 43'E). The cruise was carried out in January 1994 onboard Australia's icebreaker R/V *Aurora Australis*. Samples were collected while stopped for CTD work by filtering the ship's clean seawater supply.

low sea surface temperature and the consequent high saturation of $CO_2(aq)$. It has been assumed that availability of $CO_2(aq)$ is a major factor controlling carbon isotopic compositions of phytoplankton [e.g., *Arthur et al.*, 1985; *Hayes et al.*, 1989; *Rau et al.*, 1989; *Popp et al.*, 1989; *Jasper and Hayes*, 1990; *Hollander and MacKenzie*, 1991]. This has led to the use of stable carbon isotope measurements for reconstructing paleo-pCO_2 records [e.g., *Jasper et al.*, 1994]. However, additional factors such as temperature, light intensity, nutrient availability, species composition, growth rate, and active dissolved inorganic carbon (DIC) transport have also been suggested to be important in determining the $\delta^{13}C$ of phytoplankton [e.g., *Rau et al.*, 1992; *François et al.*, 1993; *Goericke et al.*, 1993; *Laws et al.*, 1995; *Bidigare et al.*, 1997a; *Laws et al.*, 1997; *Popp et al.*, 1998].

In this paper we examine variations in carbon isotopic composition of Southern Ocean suspended particulate organic matter, and individual compounds, some of which are exclusively derived from phytoplankton (e.g., phytol, sterols), from surface water samples collected in the Southern Ocean south of Australia. We infer the fractionation behavior of different phytoplankton as reflected in the isotopic composition of individual compounds and examine how it affects the carbon isotopic composition of bulk suspended particulate organic matter. We document isotopic variability in individual compounds of up to 10‰ in a single sample and its influence on bulk suspended organic matter isotopic compositions. We discuss the factors which contribute to this isotopic variability, among them $CO_2(aq)$ concentrations, the isotopic composition of CO_2, microalgal growth rates, algal community structure, and details of the physical oceanographic environment. Our general hypothesis is that fractionation varies as a function of $CO_2(aq)$ concentration, algal growth rates, and

community structure. We speculate on the implications of these results for interpreting the $\delta^{13}C$ of suspended particulate and sedimentary organic materials.

2. Materials and Methods

Samples used for this study were collected from the locations shown in Figure 1 on a cruise of the R/V *Aurora Australis* from January to March 1994, along the WOCE SR3 line (Hobart to Antarctica) and along a section across the Princess Elizabeth Trough (PET), from the West Ice Shelf to the Kerguelen Plateau. Samples of suspended particulate organic matter (SPOM) were collected every ~30 nautical miles, while the ship was stopped, along the transects from the ship's uncontaminated seawater system onto precombusted glass fiber filters (143 mm diameters Gelman A/E) using an in-line filter apparatus. Along the SR3 line, 42 SPOM samples were collected at stations between 45° and 65°S; across the PET, 17 samples were collected at stations between 58° and 67°S (Table 1). All SPOM samples were filtered from 160-200 L of water, immediately frozen and stored frozen until analysis.

Physical oceanographic measurements, carbon analyses ([DIC], fCO_2, alkalinity), biological studies (fluorescence profiles, nutrient analyses, plankton counts, and pigment analyses) were also performed. Surface water fCO_2 was continuously monitored from the ship's uncontaminated seawater system and [$CO_2(aq)$] calculated from fCO_2, temperature, and salinity, after *Weiss* [1974]. The fCO_2 measurements were made by circulating air, which had equilibrated with a shower of water from the uncontaminated seawater line, through a infrared gas analyzer (LICOR Model 6252) [*Metzl et al.*, 1999]. The air was dried prior to analysis, and standards referenced to the World Meteorological Organization (WMO) X85 mole fraction scale were used to calibrate the analyzer. The fCO_2 data were corrected for warming between the seawater inlet in the ship's bow (water depth ~5 m) and the equilibration chamber after *Copin-Montegut* [1988, 1989]. The concentrations of total dissolved inorganic carbon were determined coulometrically using a Single-Operator Multi-Metabolic Analyzer (SOMMA) system similar to that described by *Johnson et al.* [1993]. Phosphate, silicate, and nitrate plus nitrite were measured using the colormetric techniques of *Strickland and Parsons* [1972] on a Alpkem "Flow Solution" Autoanalyzer continuous flow system. Unfortunately, for reasons specific to the autoanalyzer sample sequence protocol [*Rosenberg et al.*, 1995], reliable surface bottle phosphate concentration determinations were rare on this voyage, whereas silicate and nitrate plus nitrite were successfully determined in nearly all surface water samples. For this reason, in considering phosphate utilization, we primarily rely on estimates from surface bottle nitrate+nitrite concentrations assuming Redfield stoichiometry (N/P=16 (by atoms), Table 1), an approximation which involved little uncertainty when compared to phosphate determinations on samples collected deeper in the mixed layer (50-75 m). Salinity was determined using a YeoKal Mark 4 salinometer standardized with IAPSO P-series salinity standards following WOCE guidelines. Microscopic algal identifications and counts were done onboard. Chlorophyll *a* analyses were done on shore by high-pressure liquid chromatography using particles from 2 L seawater samples filtered through glass fiber filters (Whatman GF/F) stored in liquid nitrogen [*Wright and Jeffrey*, 1997].

Table 1. Sample Location and Results from Chemical and Bulk Isotopic Analyses

Sample	Lat., °S	Long., °E	Vol. Filtered, L	T, °C	Salinity	fCO_2, μatm	$CO_2(aq)$, μmol kg⁻¹	NO_3+NO_2, μM	$Si(OH)_4$, μM	PO_4,[b] μM	$\delta^{13}C_{CO_2}$,[c] ‰	$\delta^{13}C_{SPOM}$, ‰	ε_P,[a] ‰
								WOCE SR-3 Section					
1	45.88	145.51	200	11.48	34.68	314	13.0	7.5	2.3	0.55	-7.29	-22.91	15.99
2	46.51	145.20	200	11.27	34.64	313	13.1	8.0	1.4	0.66	-7.35	-20.63	13.56
3	46.96	144.97	200	10.33	34.40	315	13.2	8.5	1.6	0.76	-7.47	-20.42	13.22
4	47.64	144.63	150	9.97	34.42	323	13.8	11.2	1.8	0.85	-7.70	-21.17	13.76
5	48.30	144.30	180	9.62	34.31	328	14.5	12.8	3.1	0.89	-7.85	-21.24	13.68
6	48.77	144.07	200	9.73	34.32	330	14.6	13.5	3.0	0.93	-7.89	-20.57	12.94
7	49.27	143.82	200	9.90	34.45	325	14.3	11.4	3.0	0.89	-7.72	-21.93	14.52
8	49.75	143.58	160	9.68	34.44	329	14.6	11.8	2.1	0.87	-7.78	-21.46	13.98
9	50.24	143.34	175	9.75	34.52	326	14.4	10.9	2.7	0.85	-7.70		
10	50.77	143.07	230	8.91	34.32	326	14.8	13.6	2.9	0.96	-7.98	-21.60	13.92
11	51.04	142.94	200	8.43	34.26	337	15.6	15.8	4.4	1.13	-8.19	-22.81	14.96
12	51.43	142.74	160	7.34	34.02	351	16.9	19.5	6.5	1.35	-8.56		
13	51.90	142.51	160	6.84	33.96	348	17.0	20.6	4.4	1.40	-8.69	-24.64	16.35
14	52.26	142.33	170	5.28	33.84	347	17.9	23.1	7.4	1.55	-9.02	-26.67	18.13
15	52.67	142.13	130	5.46	33.86	345	17.7	23.1	1.9	1.56	-9.00	-25.23	16.65
16	53.15	141.89	201	5.43	33.85	341	17.5	22.6	1.8	1.63	-8.97	-25.99	17.48
17	53.58	141.67	200	4.61	33.89	342	18.1	23.9	1.9	1.56	-9.14	-26.37	17.69
18	54.06	141.44	200	4.42	33.88	350	18.7	25.4	3.4	1.57	-9.27	-26.43	17.62
19	54.52	141.21	200	4.82	33.87	359	18.9	25.5	5.6	1.74	-9.24	-26.53	17.76
20	55.06	140.94	200	4.52	33.88	355	18.8	25.6	5.3	1.82	-9.28	-27.35	18.58
21	55.49	140.72	200	4.62	33.89	351	18.6	24.6	4.5	1.67	-9.20	-27.16	18.47
22	55.93	140.50	200	5.09	33.90	357	18.6	25.3	3.2	1.59	-9.20	-26.76	18.04
23	56.44	140.25	205	5.24	33.91	368	19.0	25.0	8.0	1.81	-9.17	-26.39	17.69
24	56.92	140.01	200	4.75	33.90	365	19.1	25.1	5.7	1.78	-9.22	-27.60	18.90
25	57.38	140.00	202	4.25	33.90	356	19.0	25.3	5.5	1.77	-9.29	-27.28	18.50
26	57.87	140.00	200	4.08	33.89	360	19.4	25.4	6.4	1.75	-9.31	-26.99	18.17
27	58.35	140.00	205	3.48	33.89	352	19.4	25.8	6.5	1.93	-9.40	-26.63	17.70
28	58.86	140.00	200	3.46	33.90	358	19.7	26.1	8.5	1.72	-9.42	-27.27	18.35
29	59.35	140.00	200	3.34	33.89	356	19.7	26.4	8.7	1.88	-9.45	-27.22	18.26
30	59.86	140.00	200	2.79	33.92	353	20.1	25.9	8.0	1.71	-9.47	-26.82	17.82
31	60.37	140.00	200	2.17	33.94	363	21.0	27.6	22.7	1.73	-9.66	-27.53	18.37
32	60.86	140.00	200	2.06	33.94	359	20.9	27.2	17.5	1.77	-9.64	-26.44	17.25
33	61.35	140.00	200	2.11	33.94	371	21.6	27.9	23.0	1.81	-9.69	-27.31	18.11
34	61.85	140.00	200	1.32	33.80	368	22.0	28.0	32.4	1.89	-9.78	-28.27	19.03
35	62.35	140.00	200	1.06	33.81	382	23.1	28.1	46.6	1.94	-9.82	-29.71	20.50
36	62.84	140.00	200	0.85	33.76	383	23.4	29.6	45.4	2.13	-9.95	-30.48	21.18
37	63.35	140.00	200	0.85	33.55	384	23.4	29.0	54.9	2.19	-9.90	-29.81	20.52
38	63.87	140.00	200	0.54	33.70	368	22.7	27.9	52.4	1.89	-9.85	-28.61	19.31
39	64.28	140.00	200	-0.72	33.39	354	22.8	27.8	59.5	1.92	-9.98	-28.52	19.09
40	64.82	140.00	170	-1.32	33.68	329	21.8	27.0	57.6	2.00	-9.97		
41	65.08	140.00	180	-1.04	33.68	333	21.8	26.6	58.5	1.83	-9.91	-28.37	18.99
42	65.40	140.00	100	-1.24	33.88	335	22.0	27.0	61.7	2.08	-9.96	-29.36	19.98

Table 1. (continued)

Sample	Lat., °S	Long., °E	Vol. Filtered, L	T, °C	Salinity	fCO_2, µatm	$CO_2(aq)$, µmol kg⁻¹	NO_3+NO_2, µM	$Si(OH)_4$, µM	PO_4,[b] µM	$\delta^{13}C_{CO_2}$,[c] ‰	$\delta^{13}C_{SPOM}$, ‰	$^{1}\varepsilon_p$,[a] ‰
Princess Elizabeth Trough Section													
43	66.32	84.72	125	-0.13	31.76	217	14.4	17.2	46.4	1.08	-8.82	-22.53	14.03
44	66.15	85.01	100	-1.31	33.08	227	15.0	18.2	46.0	1.14	-9.03	-23.05	14.35
45	65.90	85.41	100	-1.16	33.18	227	15.0	18.4	46.8	1.15	-9.03	-22.16	13.42
46	65.82	85.42	140	-1.24	33.23	227	15.0	18.5	47.6	1.16	-9.05	-22.16	13.41
47	65.75	85.41	143	-1.28	33.21	231	15.3	18.7	48.3	1.17	-9.07	-21.95	13.16
48	65.55	85.40	140	-0.41	33.47	241	15.5	18.3	54.0	1.14	-8.95	-24.20	15.63
49	65.09	85.32	170	0.03	33.65	279	17.6	23.3	46.9	1.46	-9.35	-26.80	17.93
50	64.62	84.98	180	0.93	33.69	344	21.1	26.0	37.7	1.63	-9.50	-26.98	17.96
51	64.16	84.59	202	1.10	33.83	362	21.9	27.5	34.6	1.72	-9.62	-28.16	19.08
52	63.72	84.13	200	1.20	33.84	360	21.6	26.7	34.3	1.67	-9.54	-27.96	18.95
53	63.29	83.75	200	1.12	33.76	337	20.3	23.4	23.5	1.46	-9.25	-27.30	18.56
54	62.75	83.47	200	1.37	33.84	325	19.4	23.4	21.7	1.46	-9.22	-27.23	18.51
55	62.16	83.28	200	1.45	33.79	282	16.8	21.3	12.7	1.33	-9.03	-28.01	19.53
56	61.44	82.97	160	1.51	33.82	288	17.1	21.0	12.1	1.31	-8.99	-28.58	20.16
57	60.96	82.78	180	1.62	33.78	283	16.8	20.7	11.4	1.29	-8.95	-28.71	20.34
58	59.97	82.37	140	1.71	33.93	310	18.3	21.8	14.7	1.36	-9.04	-27.37	18.84
59	58.96	82.03	102	1.62	33.95	329	19.4	25.3	24.8	1.58	-9.37	-25.37	16.42

Lat., latitude; Long., longitude; Vol., volume.

[a] ε_p determined from bulk SPOM assuming $\delta_{SPOM} = \delta_{phytoplankton}$; see text.

[b] Phosphate concentrations for PET calculated (NO_3+NO_2) assuming Redfield N/P = 16; see text.

[c] Determined from $\delta^{13}C$-DIC modeled after Broecker and Maier-Reimer [1992]; see text.

Microalgal growth rates were estimated in two ways from (1) the temperature, light, and nutrient dependent model of *Six and Maier-Reimer* [1996] and (2) shipboard ^{14}C uptake experiments [*Mackey et al.*, 1995]. The first assumes the temperature-growth relationship of *Eppley* [1972], Michaelis-Menten nutrient dependence (half-saturation at 0.016 μM phosphate), and represents photosynthetically active radiation (PAR) as the average over the mixed layer of the exponentially attenuated surface irradiance. Community microalgal growth rates were calculated by combining mixed layer depth estimates from shipboard conductivity-temperature-depth (CTD) temperature and salinity profiles, with surface irradiance estimates for January 1991 from the model of *Bishop and Rossow* [1991], available at http://www.giss.nasa.gov/data/seawifs/data (data for 1994 is not yet available and the 1991 data were typical of the 8 years processed to date). Mixed layer column growth rates were estimated also from shipboard short-term (1 hour) ^{14}C production versus irradiance (the so-called, P versus E) experiment) carried out on samples from several depths, combined with chlorophyll-calibrated fluorescence profiles [see *Mackey et al.*, 1995], and, like the Six and Maier-Reimer model, with mixed layer depths estimated from CTD profiles and irradiances from the model of *Bishop and Rossow* [1991]. Ten percent respiration loss and a carbon/chlorophyll a ratio of 50 (weight/weight) were assumed in order to calculate net production and thus growth rates.

No measurements of the isotopic composition of total dissolved CO_2 (δ^{13}C-DIC) are available; therefore δ^{13}C-DIC was calculated using the model of *Broecker and Maier-Reimer* [1992]. This model assumes that δ^{13}C-DIC can be estimated from dissolved phosphate concentrations and a constant difference between the isotopic compositions of DIC and phytoplankton (assumed here to be 20‰). Modeled variations in δ^{13}C-DIC (Table 1) agree well with historical observations for the Southern Ocean [see *Lynch-Stieglitz et al.*, 1995; *François et al.*, 1993]. The isotopic composition of CO_2(aq) was determined from δ^{13}C-DIC and the relative abundances of carbonate species. The latter was determined from concentrations of DIC, phosphate, silicate, and fCO$_2$ following *Millero* [1995]. The dissociation constants for carbonic and boric acids used in this calculation were from *Dickson* [1990a, b] and *Roy et al.* [1993] and corrected for the effects of pressure using *Millero* [1979]. The potential error involved in using modeled δ^{13}C-DIC values is difficult to assess; although, it is likely to be small relative to variation in the isotopic composition of organic materials. A subsample of each filter was prepared for bulk δ^{13}C analyses using methods of *Wedeking et al.* [1983] after acid fuming (HCl 50% vol/vol for 12 hours).

Filters containing SPOM were processed for compound identification and compound-specific isotopic analysis at the Skidaway Institute of Oceanography using procedures described by *Wakeham and Canuel* [1988]. Approximately half of the samples collected along the WOCE SR3 section and all of the PET samples were processed. Briefly, the filters were Soxhlet extracted with methylene chloride:methanol (2:1, vol/vol), and extractable lipids were partitioned into methylene chloride after addition of the 5% NaCl solution. Neutral and acidic lipids were separated by saponification using aqueous 0.5 N potassium hydroxide in methanol followed by serial extraction from basic solution (pH > 13) and acidic solution (pH < 2). The total neutral fraction was derivatized to trimethylsilyl-ethers with N,O-bis(Trimethylsilyl)trifluoroacetamide and analyzed directly by gas chromatography. Distributions of individual compounds and their

concentrations were obtained by addition of known quantities of an internal standard (5α(H)-cholestane) to the total neutral fraction prior to analysis by gas chromatography (GC) and computerized gas chromatography-mass spectrometry (GC/MS). Compound-specific isotopic results reported here were from duplicate or triplicate analyses by isotope-ratio-monitoring GC/MS (irmGCMS, Ultra 1, 50 m) performed at the University of Hawaii using techniques described by *Hayes et al.* [1990], *Merritt and Hayes* [1994], and *Merritt et al.* [1995]. Isotopic analyses reported in standard δ-notation in Table 2 have been corrected for the addition of carbon during derivatization. Use of compound-specific isotopic analyses for environmental interpretations requires knowledge of the relationship between the isotopic composition of the compound(s) analyzed and that of the whole organism [see *Hayes*, 1993; *Summons et al.*, 1994].

$$\varepsilon_{biomarker} \equiv (\frac{\delta^{13}C_{organism} +1000}{\delta^{13}C_{biomarker} +1000}- 1)1000$$

Following results of recent laboratory experiments [*Bidigare et al.*, 1997b; *Schouten et al.*, 1998], we adopt $\varepsilon_{sterol} = 7‰$ and $\varepsilon_{phytol} = 4‰$. We calculate isotopic fractionation (ε_P [*Freeman and Hayes*, 1992]) using standard formulation. Calculations of ε_P based on sterols and phytol include a correction for the difference between the isotopic composition of the compound and that of the whole cell which occurs during biosynthesis of the compound, i.e.,

$$\varepsilon_P \equiv (\frac{\delta^{13}C_{CO_2} +1000}{\delta^{13}C_{biomarker} +\varepsilon_{biomarker} +1000}- 1)1000$$

3. Results and Discussion

3.1. Oceanographic Setting

The samples cover the complete range of open Southern Ocean environments (Figures 2 and 3). The Southern Ocean can be divided into several broad regions separated by major oceanic fronts [*Rintoul et al.*, 1997]. From the north to the south, these include the Subantarctic Zone (SAZ) from ~40°-50°S bounded to the north by the Subtropical Convergence (STC) and to the south by the Subantarctic Front (SAF). The SAF marks the northern edge of the eastward flowing Antarctic Circumpolar Current (ACC), usually centered around 50°-51°S between 140° and 152°E and is characterized by rapid temperature and salinity changes (~8°-5°C and ~34.5 to less than 34.2, respectively) over about 30-50 nautical miles. Summer warming can often mask the change in temperature across the SAF in surface waters. The Polar Frontal Zone (PFZ) extends south from the SAF to the PF, a subsurface feature marked by the northern-most extent of cold subsurface waters (<2°C at about 200 m), typically found at about 54°S south of Australia. The Polar Zone (PZ) extends on southward to the Antarctic Divergence, which marks the transition from prevailing westerlies to coastal Antarctic easterlies, as well as the location of upwelling of circumpolar deep water. South of the Antarctic Divergence, the influence of sea-ice is large, and we refer to this region as the Seasonal Sea-Ice Zone (SSIZ). South of Australia, the PZ can be further divided into north and south zones by the presence of a southern branch of the Polar Front (PF-S). The southern branch is less clearly defined than the northern but generally occurs between 57° and 60°S. Indicators of the southern PF include the region where there is a rapid change in depth of the

Table 2. Results of Molecular and Compound-Specific Isotopic Analyses of Phytol and Major Sterols

Sample	phytol ng L^{-1}	phytol ‰	sterol I ng L^{-1}	sterol I ‰	sterol II ng L^{-1}	sterol II ‰	Sterol sterol III ng L^{-1}	sterol III ‰	sterol IV ng L^{-1}	sterol IV ‰	sterol V ng L^{-1}	sterol V ‰	ΣSterol, ng L^{-1}
WOCE SR-3 Section													
2	59	-27.0±0.1	53	-26.1±0.3	57	-26.3±0.3	41	-28.3±0.2	16	-31.1±0.3	23	-30.3±0.5	311
4	83	-26.9±0.5	85	-26.6±0.3	97	-27.4±0.5	85	-30.4±0.4	27	-33.8±1.3	25	-30.2±1.5	486
6	149	-26.1±0.1	81	-26.7±0.2	60	-25.9±0.8	80	-30.5±0.7	39	-33.6±0.2	17	-28.0±1.8	415
10	89	-26.2±0.2	65	-25.5±0.1	48	-26.1±1.2	60	-30.8±0.1	24	-33.7±0.3	10	-27.5±0.3	307
12		-29.6±0.3		-29.5±0.1		-29.9±0.4		-35.2±0.3		-33.2±0.1		-31.2±0.3	
13	73	-30.0±0.4	61	-28.8±0.3	46	-31.2±0.5	72	-34.5±0.2	30	-34.2±0.2	18	-41.1±0.3	377
16	70	-31.6±0.3	50	-31.2±0.6	50	-31.3±0.9	79	-34.9±0.4	36	-38.6±0.3	12	-41.9±0.3	401
17	65	-30.4±0.3	83	-30.0±0.1	84	-30.2±0.2	89	-36.3±0.5	57	-38.1±0.7	15	-37.5±0.4	552
20	50	-32.6±0.3	81	-31.9±1.3	125	-33.1±0.5	87	-36.2±0.1	48	-36.9±0.2	12	-34.2±0.3	551
23	35	-30.7±0.1	51	-31.3±0.3	39	-32.5±0.9	58	-37.0±0.2	28	-37.3±0.8	8	-38.7±0.3	294
25	38	-34.9±1.9	44	-33.5±2.1	35	-34.4±1.6	56	-38.7±0.9	32	-38.7±1.4	10	-41.5±0.3	296
28	53	-32.9±0.6	54	-31.3±0.5	54	-32.1±0.4	66	-38.3±0.4	42	-39.3±0.2	11	-42.4±1.1	382
30	56	-32.4±0.3	58	-30.3±0.1	44	-32.0±0.9	52	-38.2±0.5	58	-39.7±0.1	8	-42.2±1.3	336
32	29	-32.0±0.2	55	-30.5±0.2	41	-32.5±0.5	43	-39.0±0.2	33	-37.6±0.8	7	-41.9±2.5	276
34	9	-34.1±0.1	37	-31.9±0.1	23	-33.3±0.1	61	-40.5±0.1	28	-35.5±0.4	7		218
35	4	-36.4±0.4	9	-33.6±0.8	6	-32.8±1.0	17	-40.2±0.5	5	-40.3±2.1	4		65
42	35	-34.6±0.4	117	-32.3±0.2	60	-32.0±0.1	153	-39.4±0.9	65	-33.6±0.4	16		609
Princess Elizabeth Trough Section													
43	93	-30.0±0.2	350	-27.6±0.6	143	-27.2±0.5	54	-38.8±0.9	46	-34.0±0.5	7		692
44	95	-30.8±0.5	457	-28.4±0.5	189	-29.0±0.4	87	-39.9±1.2	64	-35.1±0.3	8		910
45	100	-30.3±0.5	635	-27.1±0.5	253	-26.9±0.9	78	-38.4±0.5	71	-33.0±0.1	9		1184
46	110	-29.6±0.6	668	-26.7±0.8	274	-26.8±0.5	84	-39.5±0.6	65		16		1232
47	57	-30.3±0.5	644	-27.3±0.3	239	-26.9±0.1	69	-39.2±1.1	49	-34.0±0.7	5		1100
48	39	-30.9±0.1	216	-28.8±0.4	94	-28.2±0.1	45	-39.4±0.1	29	-34.9±0.1	3		436
49	48	-33.1±0.1	178	-30.6±0.6	87	-30.3±0.1	83	-39.3±0.9	67	-34.2±0.3	7		500
50	55	-33.6±0.2	225	-31.7±0.1	108	-32.3±0.2	98	-40.1±0.1	96	-35.3±0.1	16		657
51	37	-34.0±0.4	61	-33.6±0.4	28	-33.9±0.9	65	-40.6±0.6	51	-33.2±0.4	7		269
52	27	-33.1±0.1	67	-33.2±0.1	31	-34.0±0.2	64	-40.3±0.1	55	-33.2±0.3	5		275
53	43	-34.2±0.4	74	-31.1±0.3	32	-31.9±0.5	46	-39.2±0.1	35	-34.7±0.1	35	-43.7±0.2	282
54	62	-33.8±0.3	132	-30.7±0.1	52	-31.1±0.5	62	-38.9±0.5	55	-35.5±0.3	64	-43.1±0.2	468
55	198	-35.1±0.9	251	-30.8±0.9	102	-31.7±1.1	70	-38.3±0.8	57	-35.8±1.4	261	-43.2±0.6	931
56	253	-34.6±0.4	257	-29.1±0.7	105	-30.7±0.5	71	-37.2±0.6	56	-35.1±0.8	343	-43.4±0.5	1056
57	260	-35.2±0.4	267	-30.5±0.7	103	-31.6±0.6	77	-37.2±0.5	57	-36.0±0.4	349	-43.3±0.5	1072
58	402	-33.4±0.5	576	-29.7±0.5	277	-30.4±0.3	151	-36.9±0.5	101	-34.0±0.1	519	-43.4±0.9	1991
59	109	-31.0±0.4	159	-29.9±0.4	72	-31.1±0.4	45	-38.7±0.8	43	-34.2±0.2	68	-42.9±0.2	488

Sterol Identification: I, cholesta-5,22E-dien-3β-ol; II, cholest-5-en-3β-ol; III, 24-methylcholesta-5,22E-dien-3β-ol; IV, 24-methylcholesta-5,24(28)-dien-3β-ol; and V, 24-ethyl-5α-cholesta-7-en-3β-ol. Average and standard deviation of two or more analyses. Some samples were too small to analyze isotopically and are shown as blanks.
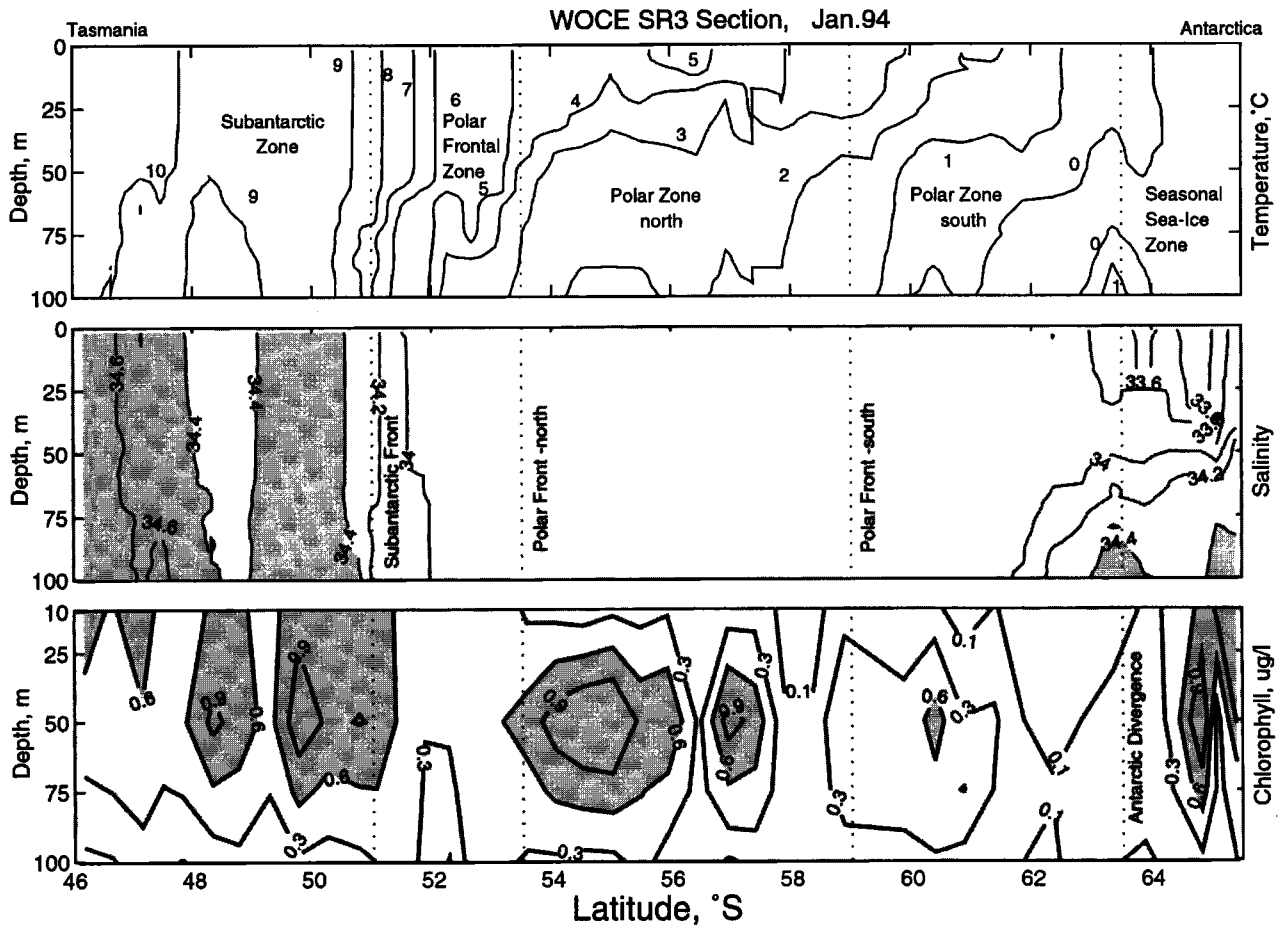
Figure 2. Distributions of temperature, salinity, and chlorophyll *a* along the SR3 transect in the top 100 m. Locations of oceanographic zones and the major fronts that divide them are shown, following *Rintoul et al.* [1997] and as described in the text. Temperature is quite uniform within the Subantarctic Zone (SAZ) and decreases across the Subantarctic Front (SAF), although seasonal surface warming broadens the thermal expression of the SAF in comparison to its north-south salinity change. The 2° isotherm marks the top of the subsurface temperature minimum layer, as well as defining the position of the Polar Front by the position of its northward extent. Salinity generally decreases from north to south. The Polar Zone (PZ) was extremely homogeneous in salinity; fresher waters formed from melting sea-ice inputs occurred near the surface in the Seasonal Sea Ice Zone (SSIZ). Upward intrusion of warm salty Circumpolar Deep Water occurred at the Antarctic Divergence (AD) (shading indicates salinities > 34.4). The relatively low salinity water (< 34.4) in the middle of the otherwise salty SAZ was the result of a large eddy which also brought cooler water into the region. The SAZ, SSIZ, and north PZ all contained relatively abundant chlorophyll *a* (shading indicates > 0.6 ug/L), with the PZ algae concentrated subsurface near the top of the colder waters. The Polar Frontal Zone and waters near the Antarctic Divergence contained very little chlorophyll *a*.

temperature minimum layer, or where there is a steep gradient in salinity in the 150-300 m depth range between water with a salinity of 34.0-34.2 to 34.6, which is characteristic of upper Circumpolar Deep Water.

All of the zones defined above can be characterized as high-nutrient, low-chlorophyll (HNLC) oceanic environments, although there are significant differences among them in terms of biological, physical, and chemical attributes. Levels of chlorophyll *a* generally decrease southward across the SAZ to the Antarctic Divergence and then increase again south of the Divergence (Figure 2). Algal distributions within the water column also vary. Note the subsurface chlorophyll maximum in the north Polar Zone along the SR3 section (Figure 2) and in the offshore portion of the PET section at the top of the winter water

layer (Figure 3). The different Southern Ocean environments exhibit both overlap and differences in typical algal communities. For example, north of the SAF, coccolithophores are relatively common but are much less so south of the SAF and particularly in the diatom-dominated Polar and Seasonal Sea-Ice Zones. These biological variations are accompanied by changes in nutrient element abundances. Of particular note is that while nutrient levels generally increase southward, nitrate levels increase strongly across the SAF, but silicate levels remain low much farther south, until the southern branch of the PF is reached (Table 1). Zonal homogeneity is of course only a first approximation to Southern Ocean environments, and there are also significant differences between the SR3 and PET sections. These include differences in water mass temperature-salinity compositions, deep
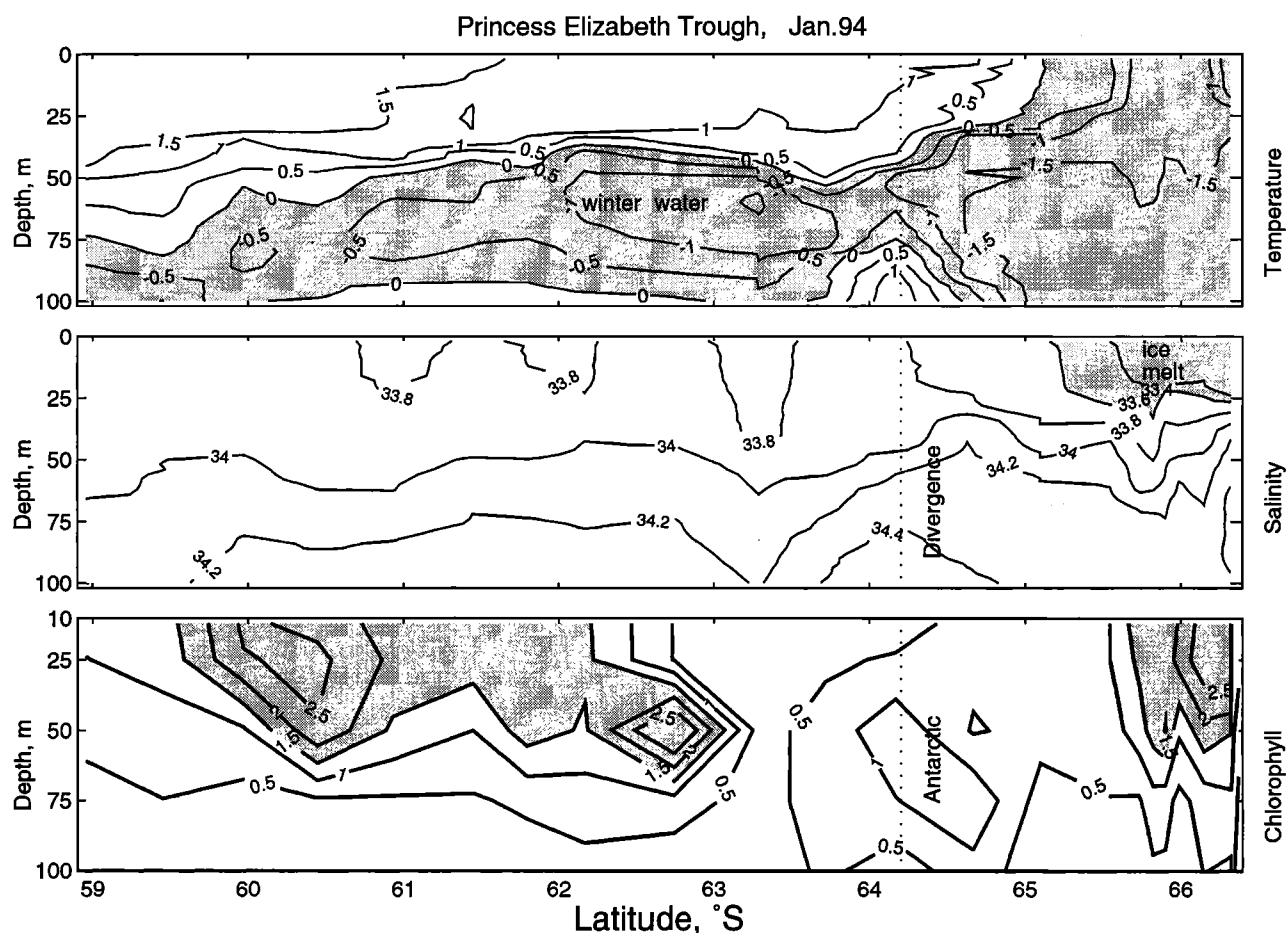
Princess Elizabeth Trough, Jan.94

Figure 3. Distributions of temperature, salinity, and chlorophyll a along the PET transect in the top 100 m. Surface waters varied from nearly 2°C in the north to the freezing point in the SSIZ. Remnant subzero winter water (shaded) underlies the entire section at ~50 m depth, effectively isolating surface waters. In the SSIZ, melting sea-ice observed during the cruise produced salinities below 33.6 (shaded). As in the SR3 section, relatively warm salty water intrudes upward into the mixed layer at the Antarctic Divergence (dotted line). Chlorophyll a levels were elevated (shading indicates >2.5 ug/L) in both the northerly shallow relatively warm surface waters and near the ice edge, with much lower levels at the AD. North of the AD, the algae were concentrated subsurface at the top of the remnant winter water.

as well as surface water nutrient concentrations, local circulation patterns including sea-ice drift, and mixed layer depths. Full details of these variations are beyond the scope of this paper; those pertinent to carbon isotopic variations are discussed further in section 3.2. Recent discussions include *Rintoul et al.* [1997], *Wong et al.* [1998], and *Worby et al.* [1998].

Concentrations of CO_2(aq) in surface waters along the SR3 line vary from 13.1 to 23.5 μmol kg^{-1}, are near equilibrium with the atmosphere, and vary mainly as a function of temperature (Figure 4) except near the retreating ice edge where enhanced phytoplankton production likely caused a drawdown of CO_2(aq), consistent with lower phosphate concentration. The $[CO_2(aq)]$ along the PET transect vary from 14.6 to 22.0 μmol kg^{-1} and are generally below that expected for equilibrium with atmospheric CO_2 (Figure 4). Unlike the majority of SR3 results, $[CO_2(aq)]$ is poorly correlated with sea surface temperature suggesting biological activity strongly influenced $[CO_2(aq)]$ along the PET transect. Several authors have suggested that the concentration of CO_2(aq) mainly controls the carbon isotopic composition of

Southern Ocean phytoplankton [e.g., *Rau et al.*, 1991a, b; *Bathmann et al.*, 1991; *Fischer*, 1991; *Dunbar and Leventer*, 1992; *Rogers and Dunbar*, 1993; *François et al.*, 1993; *Kopczynska et al.*, 1995; *Dehairs et al.*, 1997; *Fischer et al.*, 1997]. Although collected within 20 days of each other on the same voyage, $\delta^{13}C$-SPOM was related to $[CO_2(aq)]$ quite differently in the two sections (Figure 4). Along the SR3 transect, $\delta^{13}C$-SPOM is negatively correlated with CO_2(aq) concentrations ($\delta^{13}C$ = -0.89$[CO_2(aq)]$ - 9.29, r^2 = 0.91, Figure 4). Similar correlations between the isotopic composition of SPOM and $[CO_2(aq)]$ have been found by *Rau et al.* [1991b], *François et al.* [1993], and *Dehairs et al.* [1997] from the Southern Ocean. In contrast, despite similar ranges of CO_2(aq) and $\delta^{13}C$ values, a poor correlation between SPOM isotopic composition and CO_2(aq) concentration was found along the PET line ($\delta^{13}C$ = -0.71$[CO_2(aq)]$ - 13.40, r^2 = 0.52, Figure 4). Because the relationship between $[CO_2(aq)]$ and $\delta^{13}C$-SPOM is so different in each of these oceanic regions, we discuss the SR3 and PET transects separately before comparing them.

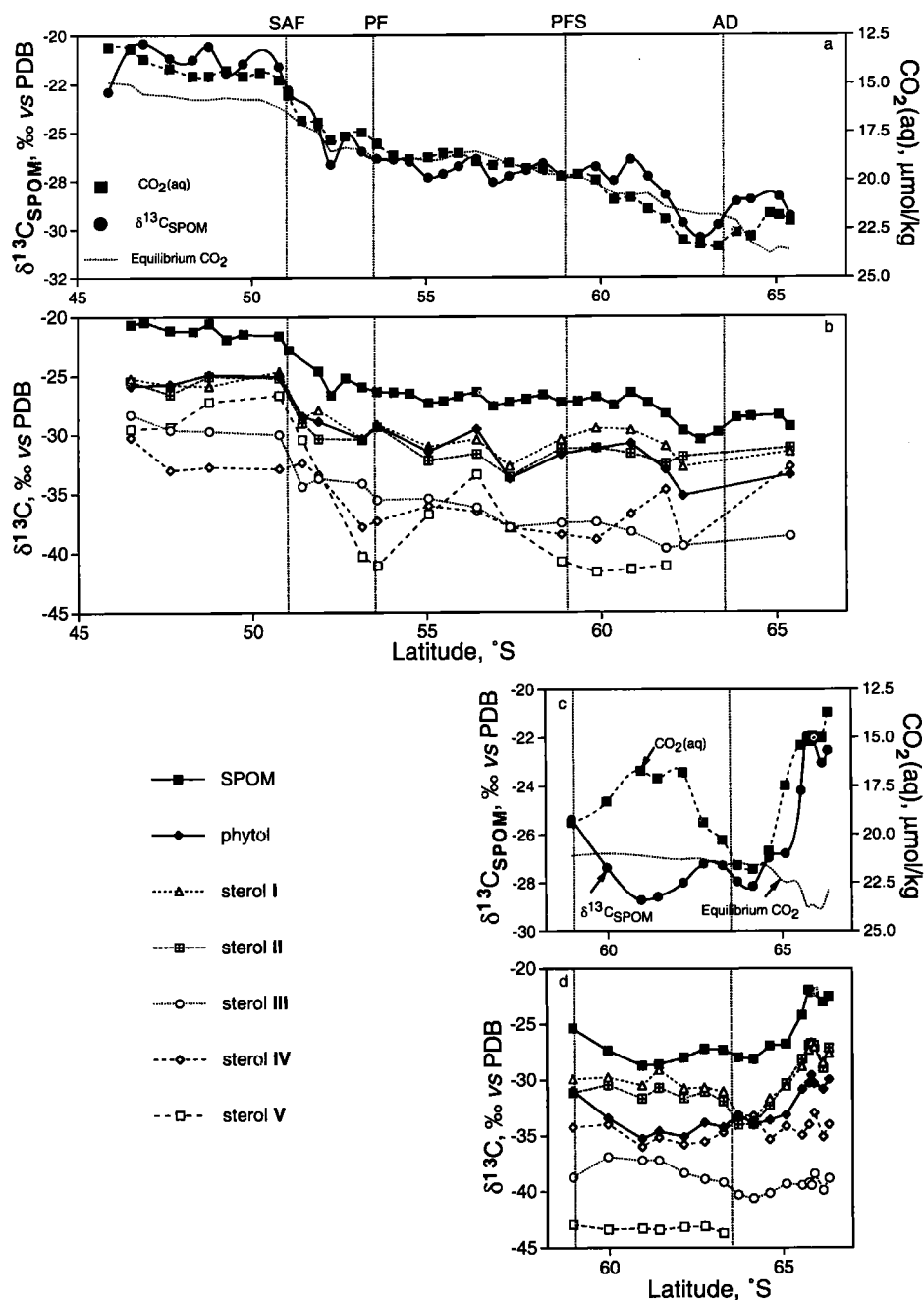**Figure 4.** Distributions of surface aqueous CO_2, $\delta^{13}C$-SPOM, and the isotopic compositions of phytol and the five major sterols. Front locations are the same as in Figure 2. CO_2 levels were generally close to atmospheric equilibrium values (dashed line) along SR3 but deviated from equilibrium in the far south and north of SR3 and in all of the PET. Individual sterol isotopic compositions, while generally decreasing southward, exhibit greater variations than those of bulk SPOM or phytol. Sterol I, cholesta-5,22E-dien-3β-ol; sterol II, cholest-5-en-3β-ol; sterol III, 24-methylcholesta-5,22E-dien-3β-ol; sterol IV, 24-methylcholesta-5,24(28)-dien-3β-ol; sterol V, 24-ethyl-5α-cholest-7-en-3β-ol.

3.2. WOCE SR3 Transect

Although the [CO_2(aq)] can explain a large amount of the variation in $\delta^{13}C$ of SPOM along the SR3 transect, variability in the carbon isotopic composition of individual compounds along these transects (Figure 4) indicate that other factors affect the $\delta^{13}C$-SPOM. Recent results of modeling [*Goericke et al.*, 1994;

Rau et al., 1996, 1997] and laboratory experiments [*Laws et al.*, 1995; 1997; *Bidigare et al.*, 1997a; *Popp et al.*, 1998] suggest that microalgal growth rate and cell size and shape also contribute to the carbon isotopic composition of phytoplankton, essentially as a balance of CO_2 supply and demand. Contributions from heterotrophic carbon sources can also play a role [*Fry*, 1988; *Hayes*, 1993; *Kenig et al.*, 1994]. We now examine these factors
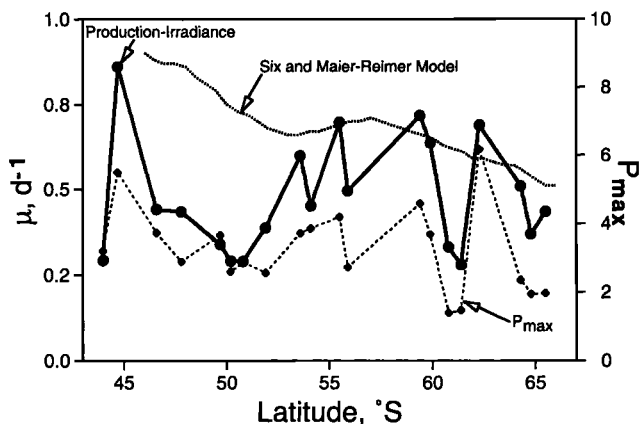
Figure 5. Comparison along the SR3 section of community phytoplankton mixed layer growth rates from shipboard ^{14}C-based production versus irradiance experiments with those predicted from temperature, light, and major nutrient distributions using the model of *Six and Maier-Reimer* [1996]. Also shown are production rates at saturating irradiance (P_{max} values) from the 10 m depth shipboard samples.

from measurements of algal growth rates, community structure, and biomarker compound abundances and isotopic compositions.

3.2.1. Growth rates. The model of *Six and Maier-Reimer* [1996] predicts growth rates ranging from 0.5 to 0.9 d^{-1}, which decrease to the south and are controlled mainly by temperature (Figure 5). Mixed layer depth variations (of typically 40-125 m) play a secondary role, followed by cloud cover driven irradiance variations. High surface water phosphate concentrations (Table 1) preclude phosphate growth limitation in the model despite the relatively high half-saturation constant. The model growth rates are generally higher than growth rates estimated for Southern

Ocean diatoms by various investigators during the austral summer (Table 3), as well as the shipboard ^{14}C results discussed next.

In contrast to the *Six and Maier-Reimer* [1996] model, mixed layer column growth rates estimated from shipboard ^{14}C measurements are lower, averaging 0.48 ± 0.17 d^{-1}, and exhibit no systematic change with latitude (Figure 5). Both variations in photosynthetic response (as estimated from the ^{14}C P versus E experiments) and changes in the vertical distributions of the algae in the water column (determined from the fluorescence profiles) contribute to the variations in column growth rates. For example, maximum ^{14}C uptake rates at saturating irradiances (P_{max} values at 10 m) were quite constant from 45° to 60°S, and the lower column growth rates from 49° to 52°S are primarily the result of the deeper mixed layers and algal distributions at the SAF and in the PFZ. In contrast, south of the Antarctic Divergence (~64°S), the small diatom dominated algal community exhibited relatively low P_{max} values, but their near surface location leads to column growth rates that are similar to the rest of the transect.

These observations highlight some of the issues involved in estimating growth rates appropriate to assessing ^{13}C fractionation from ^{14}C P versus E experiments. Using mixed layer column growth rates assumes that the observed vertical algal distributions, P versus E parameters, and climatological irradiances are typical of the period over which the ^{13}C compositions have been determined. It also assumes that the surface SPOM samples obtained from 10 m depth have experienced the column weighted mean growth rate, i.e. that the surface layer has indeed been well mixed over the residence time of the cells. The observations provide two ways to evaluate these assumptions. First of all, dividing column chlorophyll inventories by production rates suggests residence times (i.e. the biomass replacement e folding time) of 1-3 days, so that more than 95% of biomass will have accumulated in the past 3-9 days. This suggests that storm timescale events which deepen mixed layers and change cloud levels could be important. Comparison of clear sky irradiances

Table 3. Growth rates of Antarctic Diatoms Estimated by Various Investigators During the Austral Summer

| Reference	Growth Rates, d^{-1}	Comments
Sakahaug and Holm-Hansen [1986]	mean = 0.24 range = 0.1-0.34	Growth rates based on chlorophyll measurements in batch cultures. Scotia/Weddell Seas. Temperature = -1 to 4°C. Cultures dominated by diatoms—*Chaetoceros tortissimus* Gran, *Nitzschia, Fragilariopsis* spp. and *Thalassiosira* sp.
Spies [1987]	mean = 0.52 range = 0.26-0.92	Growth rates determined by successive cell counts on natural populations incubated in polycarbonate bottles. Weddell Sea. Temperature = -1°C *Thalassiosira, Eucampia, Chaetoceros, Rhizosoleina, Nitzschia, Thalassiothrix, Coscinodiscus* and others.
Tilzer and Dubinsky [1987]	mean = 0.14 range = 0.04-0.19	Growth rates based on C-14 incubations and assumed C:chl ratio of 50. Southern Drake Passage. Temperature = -2 to +8°C. Net plankton dominated by diatoms *Corethron criophilum, Chaetoceros* spp., *Thalassiosira* sp. and *Rhizosolenia alata*. 76% of chlorophyll in cells which pass through a 20 μm filter.
Wilson et al. [1986]	surface rates = 0.26-0.36 integrated rates = 0.10-0.15.	Growth rates determined from autoradiography and carbon estimates based on cell volume. Receding ice edge in Western Ross Sea. Mainly *Nitzschia curta* with some *Nitzschia closterium*.
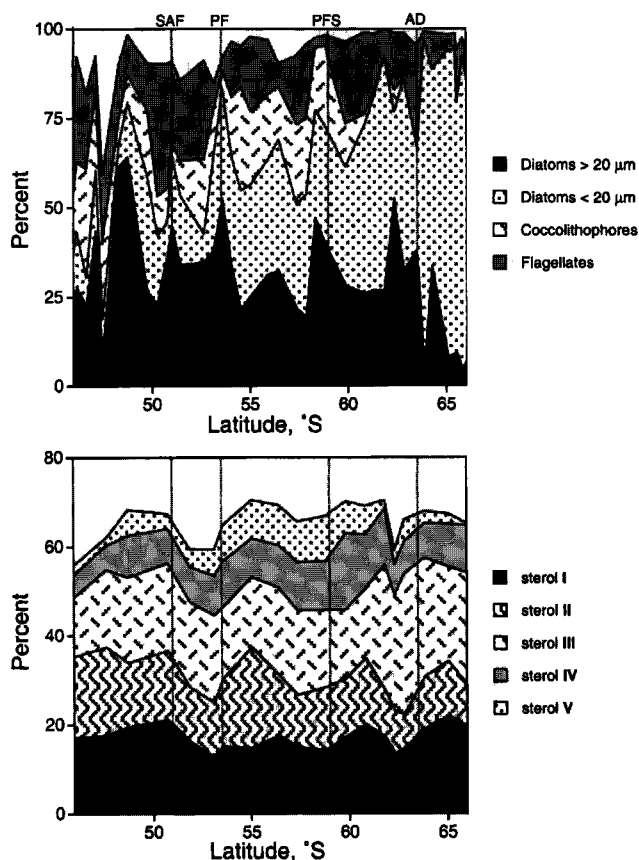
Figure 6. Distribution of cell counts and biomarker compound abundances along the SR3 section. The legends for cell counts and sterol abundances list the components in order from most to least abundant. While individual species abundances were not quantified, *Nitshia*, *Coretheron*, *Chaetocerosis*, and *Fragillariopsis* were important constituents. Individual sterol abundances generally vary little with latitude compared to the large variation in their isotopic composition (see Figure 4). Sterol I, cholesta-5,22E-dien-3β-ol; sterol II, cholest-5-en-3β-ol; sterol III, 24-methylcholesta-5,22E-dien-3β-ol; sterol IV, 24-methylcholesta-5,24(28)-dien-3β-ol; sterol V, 24-ethyl-5α-cholest-7-en-3β-ol.

with cloud-covered values suggests irradiance changes would not exceed a factor of 2 [*Bishop and Rossow*, 1991]. For typical light attenuation lengths of ~40 m, storm-driven deepening of an initially very shallow mixed layer from 20 to 100 m would decrease mean light levels two-fold, with similar misestimation of growth rate. Second, because growth rates estimated from the 10 m bottle samples alone (not shown) are very similar to the column growth rate, and because profiles of algal community compositions show little variation with depth (H. Marchant, unpublished observations, 1994), the assumption that the 7 m depth underway SPOM sampling obtained algae which experienced the column weighted mean growth rate appears well justified.

Overall the ^{14}C-based growth rates appear appropriate for assessing growth rate contributions to ^{13}C fractionation, although the methodology is not without uncertainties (see review by *Sakshaug et al.* [1997]). For example, the possibility exists that

carbon/chlorophyll ratios changed systematically with latitude, although we have neither any reason to expect this nor any data to rule it out. We used a shipboard estimate of carbon/chlorophyll which is slightly lower than the average from the literature [*Sakshaug and Holm-Hansen*, 1986; *Figueiras et al.*, 1994; *Smith et al.*, 1996; *DiTullio and Smith*, 1996], but the uncertainty is rather large (> 30%). Because the ^{14}C based growth rates correspond to estimates of Southern Ocean diatoms (Table 3) better than those predicted from the *Eppley* [1972] temperature dependence of the *Six and Maier-Reimer* [1996] model, the simplest conclusion remains that growth rates were reasonably independent of latitude, temperature, and CO_2(aq) concentrations along the SR-3 transect in January 1994 (although this may not be true in other seasons). This interpretation implies that variations in microalgal growth rates contributed only variance to the observed correlation of δ^{13}C-SPOM with CO_2(aq), rather than influencing its average nature. In fact, latitude by latitude comparison of the sparse ^{14}C-based growth rates with the variability of the δ^{13}C-SPOM correlation with CO_2(aq) reveals no consistent effect of growth rate at all; for example, regions in which the ^{14}C data suggest relatively low growth rates (e.g. near 50° and 62°S) do not exhibit relatively low δ^{13}C-SPOM values given their CO_2(aq) concentrations. Furthermore, lower than maximum growth rates are consistent with recent data suggesting that micronutrients, in particular bioavailable iron, may exert strong controls on Southern Ocean phytoplankton growth rates [*Martin et al.*, 1990; *Banse*, 1996; *Sedwick and DiTullio*, 1997]. It appears that factors other than algal growth rates are more important in controlling the carbon isotopic composition of SPOM.

3.2.2. Community Structure. Effects of community structure on δ^{13}C-SPOM were evaluated by comparing distributions of flora (microscopic cell counts) with the concentration and isotopic composition of algal biomarkers. Importantly, δ^{13}C-phytol and δ^{13}C-SPOM values are well correlated ($\delta^{13}C_{phytol} = 1.15 * \delta^{13}C_{SPOM} - 0.86$, $r^2 = 0.91$) with a mean difference of 4.7±1.2‰ (Tables 1 and 2), a result expected since all oxygenic photoautotrophs produce chlorophyll a, the major source of phytol and SPOM. The mean difference is slightly higher than that obtained from phytoplankton cultures (~4‰ [*Hayes*, 1993; *Bidigare et al*, 1997b; *Shouten et al.*, 1998]), but is consistent with minimal heterotrophic contributions to δ^{13}C-SPOM [see *Fry and Sherr*, 1984]. However, phytoplankton community changes do play an important role in controlling ϵ_p.

Diatoms dominate the flora along most of the SR-3 transect (Figure 6). Large diatoms (>20 μm) make up ~30% of the counted cells throughout the transect. Small diatoms (<20 μm) increase steadily southward from very low levels (~5%) north of the SAF to 10% in the PFZ, 25% in the PZ and reach 80-90% south of the Antarctic Divergence in the SSIZ. Coccolithophores also exhibit very low levels north of the SAF and increase southward, reaching relative abundances of ~20% in the PFZ and PZ before disappearing further south. Flagellates exhibit a maximum of ~20% in the PFZ, contribute ~15% in the PZ, but are present in very low abundances in both the far north (SAZ) and far south (SSIZ).

Five major sterols, four known to occur in diatoms [e.g., *Volkman*, 1986], comprise ~60% of the sterols along the SR-3 transect. One of the five, 24-methylcholesta-5,22E-dien-3β-ol (sterol III), exhibits a small increase in the SSIZ in the far south where small diatoms dominate (Figure 6), and a less abundant
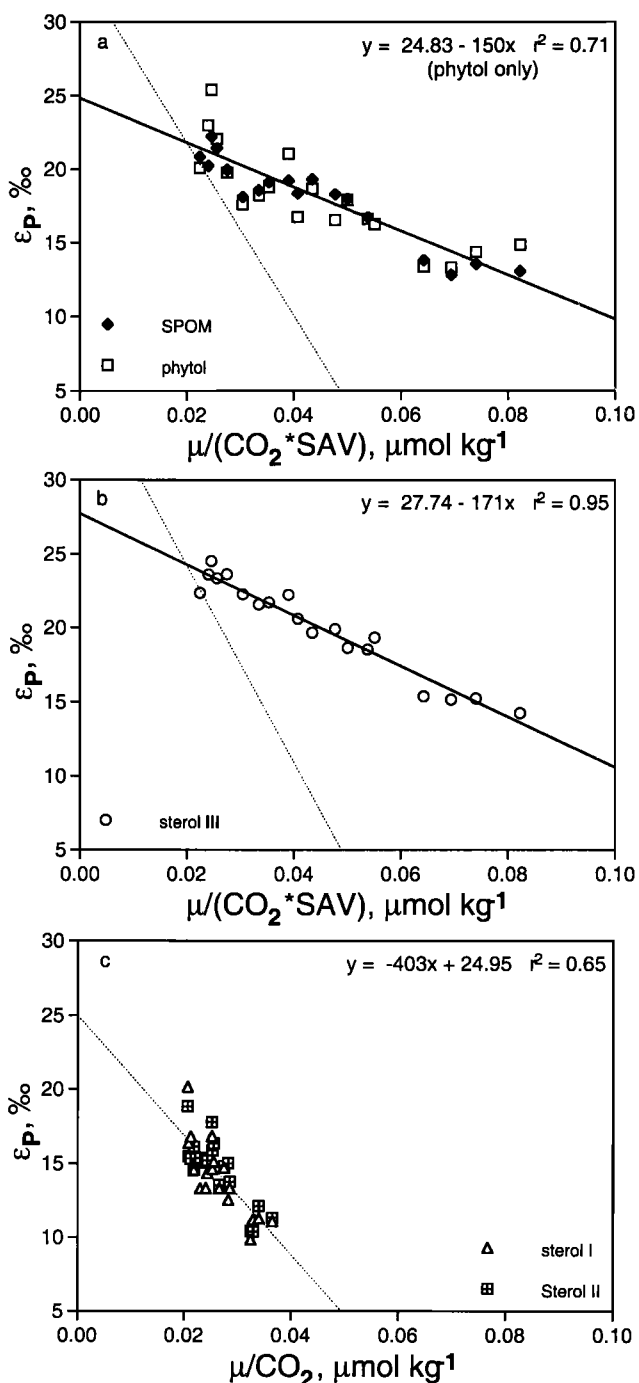
Figure 7. Assessment of the role of community structure variations along the SR3 transect. Solid lines show regression analysis for ε_p versus $\mu/(CO_2*SAV)$, whereas dotted lines show regression analysis for ε_p versus μ/CO_2. Consideration of the mean diatom surface area/volume ratio change with latitude (SAV) for phytol, SPOM, and sterol III decreases the slope of the regression and yields an intercepts consistent with results of laboratory experiments suggesting changes in community structure influence fractionation of phytol, SPOM, and sterol III. Regression of ε_p onto μ/CO_2 for sterols I and II yields an intercept consistent with results of laboratory experiments suggesting changes in community structure do not affect the isotopic composition of these sterols. The ε_p values for sterols IV and V are poorly correlated with μ/CO_2 implying that these biomarkers are derived from a variety of organisms across the section (data not shown).

sterol, 24-ethyl-5α-cholest-7-en-3β-ol (sterol V), shows doubled relative concentrations in the PZ where cocolithophores increase similarly, although there are no reports of this latter compound in *Emiliania huxleyi*, the dominant cocolithophore in this region [see *Sikes et al.*, 1997]. In general, the sterol relative abundance exhibits much less variation with latitude than the organism counts (Figure 6). This suggests that several of the organism classes (at least the small and large diatoms certainly) contribute to the production of the major sterols and with similar relative sterol abundances in each organism class. In contrast, individual sterol isotopic compositions change with latitude more significantly than their relative concentrations, and in different ways than those of either SPOM or phytol. The isotopic composition of sterol III exhibits a trend toward progressive depletion in ^{13}C relative to phytol toward the south, despite its relatively invariant fractional abundance (Figures 3 and 6). Comparison to the cell counts suggests the simplest interpretation is that it is produced by both the large and small diatoms and that the smaller diatoms, which increase in relative abundance to the south, are the dominant source of this molecule in the south.

To evaluate the role of community structure in controlling $\delta^{13}C$ compositions, ε_p was calculated for SPOM, individual sterols, and phytol, and the relationships between ε_p, μ, and [CO_2(aq)] were then compared with results of recent laboratory experiments [*Laws et al.*, 1995, 1997; *Bidigare et al.*, 1997a; *Popp et al.*, 1998] which found that a supply versus demand model for CO_2 uptake and associated isotopic fractionation could describe a wide range of algal species isotopic compositions if cell size and shape variations were taken into account. For this comparison we assumed $\varepsilon_{biomarker}$ values of +4‰ for phytol and +7‰ for the sterols; the modeled isotopic compositions of DIC and that demand for CO_2(aq) by the cell was constant and is represented by phytoplankton growth rate ($\mu = 0.48$ d^{-1}). As noted previously [*François et al.*, 1993], isotopic variations in DIC account for a small fraction of the variation in ε_p. The ε_p values for 24-methylcholesta-2,24(28)-dien-3β-ol (IV) and 24-ethyl-5α-cholest-7-en-3β-ol (V) are poorly correlated with μ/CO_2 implying that these biomarkers are derived from a variety of organisms across the section (data not shown). However, ε_p for SPOM, phytol, and the remaining sterols are well correlated with μ/CO_2; however, the slope and intercept of the lines describing these data are quite different.

Several authors have recognized that the supply of CO_2 to a microalgal cell is affected by [CO_2(aq)] and cell size [*François et al.*, 1993; *Goericke et al.*, 1993; *Laws et al.*, 1995; *Rau et al.*, 1996], and recently, *Popp et al.* [1998] showed that the slopes of the lines describing relationships between ε_p and $\mu/[CO_2$(aq)] for eukaryotic algal species are a direct function of differences in the surface area and volume of microalgal cells. In addition, for eukaryotic algae, *Popp et al.* [1998] showed in the limit as μ/CO_2 → 0 that ε_p should approach ε_f, the maximum fractionation associated with the flux-weighted average of all carbon-fixing reactions in the cells. Maximum fractionations of 25-28‰ have been suggested by *Raven and Johnson* [1991] and by *Goericke et al.* [1994]. To determine if cell surface area and volume changes contributed to the relationship between ε_p and μ/CO_2 across the SR3, we considered changes in the mean cell size of the dominant diatom flora as a function of latitude as determined by light microscopy. It was assumed based on distributions of diatom species (H. Marchant, unpublished observations, 1994), that the counted small (<20 μm) and large diatoms (>20 μm) had equivalent spherical diameters of 2 and 16 μm, respectively.

These choices represent well the surface area and volume characteristics of the mix of distinctly nonspherical cells in the observed diatom fractions (e.g., many pennate >20 μm diatoms have lengths of 40-50 μm but widths of <10 μm). Using this approach, mean spherical diatom cell diameter changed from 13 μm in the north to 5 μm in the south indicating an increase in mean diatom cell surface area/volume ratio.

Changes in cell size and shapes with latitude affect the relationship between ε_P and μ/CO_2 for phytol sterol III significantly (Figure 7). Specifically, for phytol and sterol III, the slope of the ε_P versus μ/CO_2*SAV (where SAV is the surface area to volume ratio of the diatom) decreases three-fold and the y intercept of a linear fit to the data converges on the expected value of 25-28‰. Without consideration of changes in cell size and shape, regression analysis predicts unreasonably high values for ε_f. These results are consistent with the laboratory-derived relationship between ε_P, μ, [CO_2(aq)], and cell surface area/volume of *Popp et al.* [1998] and imply that changes in cell size had a significant influence on the isotopic composition of sterol III, phytol, and SPOM along the SR3 transect. The steep slope of ε_P versus μ/CO_2 uncorrected for SAV for cholest-5-en-3β-ol (sterol II) and cholesta-5,22E-dien-3β-ol (sterol I), and an intercept of ~25‰ are consistent with derivation of these compounds from large cells with no significant change in the mean surface/volume. The fact that the slope of the line describing the ε_P - μ/CO_2*SAV relationship for phytol is intermediate between that of sterol I/II and sterol III (Figure 7) indicates that both large and small cells contributed to phytol. In comparison to the sterol III correlation, the lower coherence of the cholesterol and phytol ε_P versus μ/CO_2 correlations (Figure 7) probably arises from contributions from a wider range of organisms including surface/volume changes, species specific growth rate variations, and possibly heterotrophic effects, although recent studies suggest very little isotopic fractionation of sterols during their incorporation by zooplankton [*Grice et al.*, 1998]. The relationships shown in Figure 7 exemplify the added value of isotopic information to biomarker approaches generally and specifically constrain the way by which community structure contributions to the phytol and δ¹³C-SPOM values can be assessed.

In summary, although the size and shapes of individual algal species along the SR3 were not determined, estimates of community cell size changes from the phytoplankton size class counts suggests both surface area/volume and [CO_2(aq)] changed roughly by a factor of 2 across the SR3 transect and thus that changes in [CO_2(aq)] and community structure were equally important in controlling the isotopic composition of phytoplankton and δ¹³C-SPOM along SR3. This result must of course be tempered by the fact that it assumes that the community growth rate estimates are representative of all the organism classes.

3.3. PET Transect

Clearly the [CO_2(aq)] explains a much smaller amount of the variation in the δ¹³C of SPOM along the PET transect in comparison to the SR3 results (Figure 4), particularly in the offshore PZ portion where low CO_2(aq) is not accompanied by ¹³C-enriched SPOM. Thus growth rate and ecosystem changes probably played a larger role than along SR3. Unfortunately, no ¹⁴C-based growth rates were determined during the PET transect. While surface temperatures varied minimally (Figure 3) so that the *Six and Maier-Reimer* [1996] model predicts relatively

constant growth, this approximation may well not be applicable, particularly given the strong changes in environmental conditions and vertical algal distributions along the PET transect. In the PZ, there was a strong subsurface chlorophyll maximum within the strong density gradient between summer-warmed surface waters and the cold winter water layer (Figure 3). This density gradient was absent in the vicinity of the Antarctic Divergence, and although chlorophyll again exhibited a subsurface maximum, abundances were much lower. South of the Antarctic Divergence melting sea-ice was present during the transect, with an associated cold and fresh, shallow stratified layer, within which algal abundances rose dramatically (Figure 3). Thus, while we have no data on growth rates, there are good reasons to expect variations. Nonetheless, while keeping in mind these caveats, it is informative to examine community structure contributions to the large range of sterol δ¹³C compositions.

Both cell counts and sterol biomarker abundances illustrate significant algal assemblage changes across the PET section (Figure 8). Small diatoms dominate the waters close to the Antarctic Divergence (AD) but give way dramatically to large diatoms both to the north in the PZ and to the south in the SSIZ. The sterol distributions also show a difference between the AD waters, where methyl-cholesterols are fairly abundant (sterols III and IV, Figure 8) and elsewhere where they are in low concentration. In addition, the sterols discriminate strongly between the PZ where sterol V is the most abundant sterol and the SSIZ where it is virtually absent. Notably sterol V was relatively rare along SR3 (Figure 6).

As in the SR3 transect, δ¹³C-phytol and δ¹³C-SPOM reflect a mix of contributions from several sources which is illustrated by their latitudinal relations to sterol isotopic compositions (Figure 4). Phytol δ¹³C again generally lies between the relatively heavy nonmethylated sterols and the lighter methyl sterols. However, in the PZ, δ¹³C-phytol is much more depleted, approaching methyl sterol values, in association with the abundant presence of the extraordinarily isotopically light 24-ethyl-5α-cholest-7-en-3β-ol (sterol V, δ¹³C approximately -43‰). The overall range of sterol isotopic compositions in the PZ is extreme, exceeding 10‰ in a single sample, and if a constant offset between sterol and phytoplankton carbon isotopic composition is assumed (ε_{sterol} =7‰, see above), it implies that algae with a wide range of cell sizes and/or growth rates contribute to δ¹³C-SPOM. Although notably, there is no suggestion of a contribution from sea-ice hosted algae even in the SSIZ, which are known to exhibit heavy δ¹³C, up to -10‰, in response to strong depletion of inorganic carbon [e.g., *Dunbar and Leventer*, 1992; *Gibson et al.*, 1999].

The source organism producing the extraordinarily isotopically light Δ⁷-sterols (sterol V) in these samples is unknown. Furthermore, Δ⁷-sterols generally have not been previously reported in any Southern Ocean organisms. Several diatoms and green algae from non-Southern Ocean locations contain low abundances of Δ⁷- and Δ⁵,⁷-sterols [*Volkman*, 1986; *Patterson*, 1992; *Volkman et al.*, 1993; *Barrett et al.*, 1995] as does a dinoflagellate, *Scrippsiella trochoidea* [*Harvey et al.*, 1988]. The Δ⁷-sterols are relatively abundant in sponges [*Voogt*, 1976; *Ballantine et al.*, 1979a, b], tunicates [*Ballantine et al.*, 1977] and holothurians [*Ballantine et al.*, 1981]. The fact that when sterol V is present the isotopic composition of phytol is affected indicates that the organism producing this compound is a photoautotroph. Large diatoms appear to dominate the flora in the region in the PET where this Δ⁷-sterol is abundant suggesting that a large
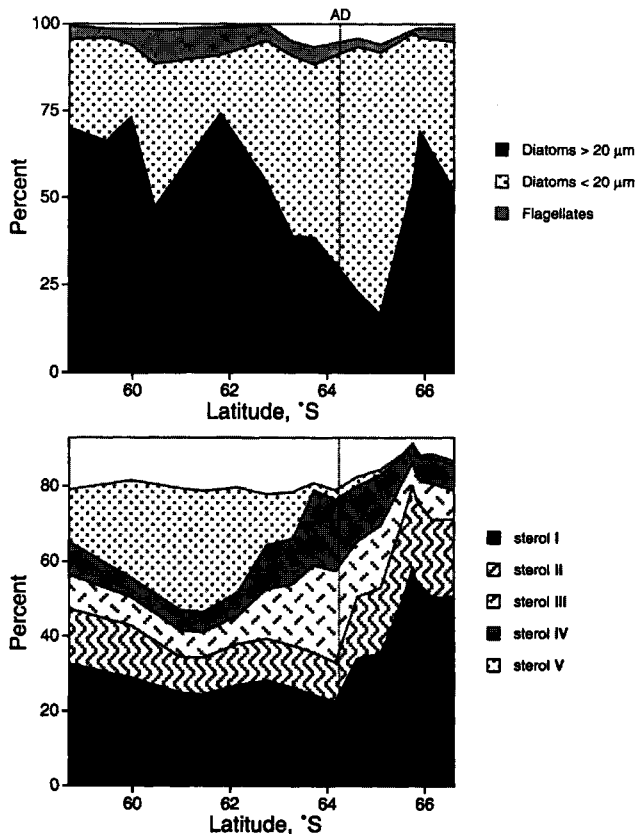
Figure 8. Distribution of cell counts and biomarker compound abundances along the PET transect. The legends for cell counts and sterol abundances list the components in order from most to least abundant. The sterol distributions also show a difference between the AD waters, where methyl-cholesterols are fairly abundant (sterol III and IV) and elsewhere where they are lower. In addition, the sterols discriminate strongly between the PZ where sterol V is the most abundant sterol and the SSIZ where it is virtually absent (sterol V was relatively rare along SR3, see Figure 6). Sterol I, cholesta-5,22E-dien-3β-ol; sterol II, cholest-5-en-3β-ol; sterol III, 24-methylcholesta-5,22E-dien-3β-ol; sterol IV, 24-methylcholesta-5,24(28)-dien-3β-ol; sterol V, 24-ethyl-5α-cholest-7-en-3β-ol.

diatom could be the source organism even though the occurrence of sterol V in Southern Ocean diatoms has not been previously noted [e.g., *Nichols et al.*, 1986, 1990, 1991, 1993; *Skerratt et al.*, 1995]. Sterol V occurred in low concentrations in samples from the WOCE SR-3 section between 52°-60°S where large diatoms are also abundant. In that region the carbon isotopic composition of sterol V was also extraordinarily depleted in ^{13}C (Figure 6). It is possible that our microscopic observations overlooked some very small cells which produced this Δ^7 sterol. However, given the unusually high abundance of this Δ^7-sterol, it is difficult to understand how the source organism could have been missed even if it was very small.

It is unclear why sterol V is so depleted in ^{13}C relative to the other compounds analyzed. Large fractionation is expected in small, slow growing phytoplankton [e.g., *François et al.*, 1993; *Goericke et al.*, 1994; *Laws et al.*, 1995; *Popp et al.*, 1998]. However, this is inconsistent with observations: Sterol V concentrations are high when large diatoms dominated the flora

and when chlorophyll *a* concentrations were high, strongly suggesting that the Δ^7-sterol was not derived from small, slow growing microalgae. Recently, *Laws et al.* [1997] showed that large fractionations can result from active transport of CO_2(aq) by diatoms. Although we have no data to show that any plankton along the PET were acquiring CO_2 by means other than diffusion, the simplest conclusion most consistent with our observations are that large diatoms grew while actively transporting inorganic carbon and synthesized sterol V. Alternatively, differences in the isotope effect associated with biosynthesis of the Δ^7 sterol ([e.g., *Schouten et al.*, 1998] could affect the calculation of ε_p and possibly invalidate the interpretation that these cells actively transported inorganic carbon. Of particular note is that whatever the source of sterol V, when this organism is abundant, it can strongly affect the isotopic composition of SPOM indicating that a single fractionation-[CO_2(aq)] global relationship [e.g., *Rau*, 1994] may not adequately describe isotopic variations in Southern Ocean phytoplankton.

Why does the PET transect display a much stronger effect of algal assemblage variations than occurred along SR3? First, the extent of nutrient utilization and biological drawdown of CO_2(aq) concentration is much greater along PET. This results from both the "bloom" conditions and the strong stratification present inshore in response to melting sea-ice inputs and offshore above an intense winter water layer. The greater "evolution" of the PET system may have led to a greater diversity of growth rates and nutrient concentrations both spatially and temporally, so that the conditions measured at the time of sampling may not represent as well those that contributed to biomass formation. Second, the PET transect is more strongly affected by coastal Antarctic oceanographic processes than the SR3 transect. Sea-ice exhibits strong offshore movement in the PET region, in contrast to the long-shore westerly drift dominant throughout East Antarctica [*Worby et al.*, 1998]. Just to the west, Prydz Bay exhibits a clockwise gyre circulation [*Wong*, 1998]. In combination these lead to an East Antarctic maximum in the seasonality of sea-ice extent in the PET region [*Worby et al.*, 1998], and a corresponding large coastal contribution to algal production processes. In contrast, circulation and sea-ice drift are dominantly zonal at the longitude of the SR3 section, confining coastal effects to a narrow band.

4. Conclusions

Using the sterol biomarker approach we have been able to sort out the relative roles of several factors contributing to the carbon isotopic composition of Southern Ocean suspended particulate organic matter. Across the open Southern Ocean along the WOCE SR3 transect in early summer, the [CO_2(aq)] plays a strong role, which is well described by a supply versus demand model for the extent of cellular CO_2 utilization and its associated linear dependence of isotopic fractionation (ε_p) on the reciprocal of CO_2(aq) concentration. Changes in algal assemblages are also important to carbon isotopic compositional changes along the SR3 transect. Their contribution is also well described by the supply and demand model, when formulated to include cell surface/volume ratio control of supply. These conclusions rely partly on the determination of essentially constant growth rates along the SR3 transect obtained from shipboard community ^{14}C primary production studies, and therefore possible growth rate variations among different algal classes could have contributed to a portion of the carbon isotopic compositional changes presently attributed to algal assemblage changes.

Along the PET transect, contributions from growth rate variations are likely given the wide range of mixed layer conditions and possible inputs of bioavailable iron from the melting ice [e.g., *Sedwick and DiTullio*, 1997]. However, the phytoplankton class counts, and presence of unusual biomarkers with extreme isotopic compositions nonetheless point to changes in algal assemblage as an important control.

These results should be used to improve the formulation of modern carbon cycle models. To date many models have approximated phytoplankton carbon isotopic fractionation as either constant [e.g., *Maier-Reimer*, 1993; *Lynch-Stieglitz et al.*, 1995] or as directly dependent on CO_2(aq) concentration [e.g., *Bacastow et al.*, 1996]. Clearly a formulation expressing ϵ_P as the reciprocal of CO_2(aq) has now emerged as the best approach [e.g., *François et al.*, 1993; *Rau et al.*, 1997; *Bidigare et al.*, 1997a; this work], and growth rate and cell size/shape effects should also be included [*Laws et al.*, 1995; *Rau et al.*, 1997; *Popp et al.*, 1998; this work].

The results are also useful to guide the study and interpretation of Southern Ocean sedimentary records. The inverse dependence of fractionation on CO_2(aq) concentrations means that cold waters with high-dissolved carbon dioxide levels will exhibit relatively low sensitivity of phytoplankton ^{13}C compositions to CO_2 changes (as noted previously by *François et al.* [1993]), and therefore growth rate and size/shape effects will need to be very carefully considered in interpretations of high-latitude sediments. Biomarker isotopic measurements will be useful in this regard to assess algal community changes generally and more specifically the possible presence of the organism responsible for the extremely ^{13}C-depleted 4-ethyl-5α-cholest-7-en-3β-ol observed in the PET section which affected δ^{13}C-SPOM so strongly. The biomarker approach using long chain alkenones which are derived almost exclusively from a few species of haptophyte algae has been very successful in warm waters [e.g., *Jasper and Hayes*, 1990; *Bidigare et al.*, 1997a], and there is a need to expand their use to the Southern Ocean. Because of the specificity of alkenones to select haptophytes [e.g., *Volkman et al.*, 1991], variations in surface area-to-volume ratio should be relatively small. *Bidigare et al.* [1997a] also showed that the carbon isotopic fractionation of alkenone-producing algae in natural marine environments varied systematically with the concentration of dissolved phosphate. These authors suggested that where both Cd/Ca and the isotopic composition of C_{37} alkadienones can be determined, it may be possible to use relationships between [PO_4] and Cd/Ca ratios in shells of planktonic foraminifera [e.g., *Mashiotta et al.*, 1997] to constrain growth rate variations and accurately estimate paleo-[CO_2(aq)], although the exact relationship between PO_4 and fractionation of the alkenone-containing haptophytes may be unique in the Southern Ocean. Since much of the algal assemblage derived variability in the ϵ_P versus $1/CO_2$(aq) relationship for Southern Ocean phytoplankton occurs in the SSIZ [this work; *Dehairs et al.*, 1997] and in the vicinity of major fronts [this work; *François et al.*, 1993, *Dehairs et al.*; 1997], the open PZ appears to be the most promising area for application of this approach for reconstructions of past surface Southern Ocean CO_2(aq) concentrations. However, even within this region, further studies of modern carbon isotopic fractionation are needed to address seasonal changes and the relationships between suspended phytoplankton and sedimented organic matter carbon isotopic compositions.

References

Arthur, M. A., W. E. Dean, and G. E. Claypool, Anomalous ^{13}C enrichment in modern marine organic carbon, *Nature, 315*, 216-218, 1985.

Bacastow, R. B., C. D. Keeling, T. J. Lueker, M. Wahlen, and W. G. Mook, The ^{13}C Suess effect in the world surface oceans and its implications for oceanic uptake of CO_2: Analysis of observations at Bermuda, *Global Biogeochem. Cycles, 10*, 335-346, 1996.

Ballantine, J. A., A. Lavis, J. C. Roberts, and R. J. Morris, Marine sterols, V, Sterols of some tunicata: The occurrence of saturated ring sterols in these filter-feeding organisms, *J. Exp. Mar. Biol. Ecol., 30*, 29-44, 1977.

Ballantine, J. A., A. Lavis, and R. J. Morris, Sterols of the phytoplankton—Effects of illumination and growth stage, *Comp. Biochem. Biophysiol., 18*, 1459-1466, 1979a.

Ballantine, J. A., A. Lavis, and R. J. Morris, Marine sterols, VII, The sterol compositions of two marine sponges: Occurrence of new C_{26} and C_{30} stanols in an oceanic sponge, *Comp. Biochem. Biophysiol. 63B*, 119-123, 1979b.

Ballantine, J. A., A. Lavis, and R. J. Morris, Marine sterols, XV, Sterols of some oceanic holothurians, *J. Exp. Mar. Biol. Ecol. 53*, 89-103, 1981.

Banse, K., Low seasonality of low concentrations of surface chlorophyll in the Subantarctic water ring: Underwater irradiance, iron or grazing?, *Prog. Oceanogr., 37*, 241-291, 1996.

Barrett, S. M., J. K. Volkman, G. A. Dunstan, and J.-M. LeRoi, Sterols of 14 species of marine diatoms (*Bacillariophyta*), *J. Phycol., 31*, 360-369, 1995.

Bathmann, U., G. Fischer, P. J. Mueller, and D. Gerdes, Short-term variations in particulate matter sedimentation off Kapp Norvegica, Weddell Sea, Antarctica: Relation to water mass advection, ice cover, plankton biomass and feeding activity, *Polar Biol., 11*, 185-195, 1991.

Bidigare, R. R., et al., Consistent fractionation of ^{13}C in nature and in the laboratory: Growth-rate effects in some haptophyte algae, *Global Biogeochem. Cycles, 11*, 279-292, 1997a.

Bidigare, R. R., B. N. Popp, F. Kenig, K. Hanson, E. A. Laws, and S. G. Wakeham, Variations in the stable carbon isotopic composition of algal biomarkers., paper presented at the 18th International Meeting on Organic Geochemistry, European Assoc. Org. Geochem., The Netherlands, 1997b.

Bishop, J. K. B., and W. B. Rossow, Spatial and temporal variability of global surface solar irradiance, *J. Geophys. Res., 96*, 16839-16858, 1991.

Broecker, W. S., and E. Maier-Reimer, The influence of air and sea exchange on the carbon isotope distribution in the sea, *Global Biogeochem. Cycles, 6*, 315-320, 1992.

Copin-Montegut, C., A new formula for the effect of temperature on the partial pressure of CO_2 in seawater, *Mar. Chem., 25*, 29-37, 1988.

Copin-Montegut, C., Corrigendum: A new formula for the effect of temperature on the partial pressure of CO_2 in seawater, *Mar. Chem., 27*, 143-144, 1989.

Dehairs, F., E. Kopczynska, P. Nielsen, C. Lancelot, D.C.E. Bakker, W. Koeve, and L. Goeyens, δ^{13}C of Southern Ocean suspended organic matter during spring and early summer: Regional and temporal variability, *Deep Sea Res., Part II, 44*, 129-142, 1997.

Dickson, A.G., Standard potential of the reaction: AgCl(s) + 1.2H$_2$(g) = Ag(s) + HCl(aq), and the standard acidity constant of the ion HSO$_4^-$ in synthetic seawater from 273.15 to 318.15 K, *J. Chem. Thermodyn., 22*, 113-127, 1990a.

Dickson, A.G., Thermodynamics of the dissociation of boric acid in synthetic seawater from 273.15 to 318.15 K, *Deep Sea Res., Part A, 37*, 755-766, 1990b.

DiTullio, G. R., and W. O. Smith, Spatial patterns in phytoplankton biomass and pigment distributions in the Ross Sea, *J. Geophys. Res.*, *101*, 18467-18477, 1996.

Dunbar, R.B., and A. Leventer, Seasonal variation in carbon isotopic composition of Antarctic sea-ice and open-water phytoplankton communities, *Antarctic. J. U.S.*, *27*, 79-81, 1992.

Eppley, R. W., Temperature and phytoplankton growth in the sea, *Fish. Bull.*, *70*, 1063-1085, 1972.

Figueiras, F. G., F. F. Pérez, Y. Pazos, and A. F. Rios, Light and productivity of Antarctic phytoplankton during austral summer in an ice edge region in the Weddell-Scotia Sea, *J. Plankton Res.*, *16*, 233-253, 1994.

Fischer, G., Stable carbon isotope ratios of plankton carbon and sinking organic matter from the Atlantic sector of the Southern Ocean, *Mar. Chem.*, *35*, 581-596, 1991.

Fischer, G., R. Schneider, P. J. Muller, and G. Wefer, Anthropogenic CO_2 in Southern Ocean surface waters: Evidence from stable organic carbon isotopes, *Terra Nova*, *9*, 153-157, 1997.

François, R., M. A. Altabet, R. Goericke, D. C. McCorkle, C. Brunetand, and A. Poisson, Changes in the δ^{13}C of surface water particulate organic matter across the subtropical convergence in the SW Indian ocean, *Global Biogeochem. Cycles*, *7*, 627-644, 1993.

François, R., M. A. Altabet, E.-F. Yu, D. M. Sigman, M. P. Bacon, M. Frank, G. Bohrmann, G. Bareille, and L. D. Labeyrie, Contribution of Southern Ocean surface-water stratification to low atmospheric CO_2 concentrations during the last glacial period, *Nature*, *389*, 929-935, 1997.

Freeman, K. H., and J. M. Hayes, Fractionation of carbon isotopes by phytoplankton and estimates of ancient CO_2 levels, *Global Biogeochem. Cycles*, *6*, 185-198, 1992.

Fry, B., Food web structures on Georges Bank from stable C, N, and S isotopic compositions, *Limnol. Oceanogr.*, *33*, 1182-1190, 1988.

Fry, B., and E. B. Sherr, δ^{13}C measurements as indicators of carbon flow in marine and freshwater ecosystems, *Contrib. Mar. Sci.*, *27*, 13-47, 1984.

Gibson, J. A. E., T. Trull, P. D. Nichols, R. E. Summons, and A. McMinn, Sedimentation of ^{13}C-rich organic matter from Antarctic sea-ice algae: A potential indicator of past sea-ice extent, *Geology*, *27*, 331-334, 1999.

Goericke, R., and B. Fry, Variations of marine plankton δ^{13}C with latitude, temperature, and dissolved CO_2 in the world ocean, *Global Biogeochem. Cycles*, *8*, 85-90, 1994.

Goericke, R., J. P. Montoya, and B. Fry, Physiology of isotopic fractionation in algae and cyanobacteria, in *Stable Isotopes in Ecology and Environmental Science*, edited by K. Lajtha and R. H. Michener, pp. 187-221, Blackwell Sci., Cambridge, Mass., 1994.

Grice, K., W.C.M Klein Breteler, S. Schouten, V. Grossi, J. W. de Leeuw, and J. S. Sinninghe Damsté, Effects of zooplankton herbivory on biomarker proxy records, *Paleoceanography*, *13*, 686-693, 1998.

Harvey, H. R., S. A. Bradshaw, S. C. M. O'Hara, G. Eglinton, and E. D. S. Corner, Lipid composition of the marine dinoflagellate *Scrippsiella trochoidea*, *Phytochemistry*, *27*, 1723-1729, 1988.

Hayes, J. M., Factors controlling the ^{13}C contents of sedimentary organic compounds: Principals and evidence, *Mar. Geol.*, *113*, 111-125, 1993.

Hayes, J. M., B. N. Popp, R. Takigiku, M. W. Johnson, An isotopic study of biogeochemical relationships between carbonates and organic carbon in the Greenhorn Formation, *Geochim. Cosmochim. Acta*, *53*, 2961-2972, 1989.

Hayes, J. M., K. H. Freeman, B. N. Popp, and C. H. Hoham, Compound-specific isotopic analyses: A novel tool for reconstruction of ancient biogeochemical processes, in *Advances in Organic Geochemistry*, *1989*, edited by B. Durand and F. Behar, pp. 1115-1128, Pergamon, New York, 1990.

Hollander, D. J., and J. A. McKenzie, CO_2 control on carbon isotope fractionation during aqueous photosynthesis: A paleo-pCO_2 barometer, *Geology*, *19*, 929-932, 1991.

Jasper, J. P., and J. M. Hayes, A carbon-isotopic record of CO_2 levels during the late Quaternary, *Nature*, *347*, 462-464, 1990.

Jasper, J. P., J. M. Hayes, A. C. Mix, and F. G. Prahl, Photosynthetic fractionation of ^{13}C and concentrations of CO_2 in the central equatorial Pacific during the last 225,000 years, *Paleoceanography*, *9*, 781-898, 1994.

Johnson, K. M., K. D. Wills, D. B. Butler, W. K. Johnson, and C. S. Wong, Coulometric total carbon dioxide analysis for marine studies: Maximizing the performance of an automated gas extraction system and coulometric detector, *Marine Chem.*, *44*, 167-188, 1993.

Kenig, F., J. S. Sinninghe-Damsté, J. W. de Leeuw, and J. M. Hayes, Molecular palaeontological evidence for food web relationships, *Naturwissenschaften*, *81*, 128-130, 1994.

Kennedy, H., and J. Robertson, Variations in the isotopic composition of particulate organic carbon in surface waters along an 88°W transect from 67°S to 54°S, *Deep Sea Res.*, *Part II*, *42*, 1109-1122, 1995.

Knox, F., and M. B. McElroy, Changes in atmospheric CO_2: Influence of the marine biota at high latitude, *J. Geophys. Res.*, *89*, 4629-4637, 1984.

Kopczynska, E., L. Goeyens, M. Semeneh, and F. Dehairs, Phytoplankton composition and cell carbon distribution in Prydz Bay, Antarctica: Relation to organic matter and its δ^{13}C, *J. Plankton Res.*, *17*, 685-707, 1995.

Kumar, N., R. Gwiazda, R. F. Anderson, and R. N. Froelich, ^{231}Pa/^{230}Th ratios in sediments as a proxy for past changes in Southern Ocean productivity, *Nature*, *362*, 45-48, 1993.

Laws, E. A., B. N. Popp, R. R. Bidigare, M. C. Kennicutt, and S. A. Macko, Dependence of phytoplankton carbon isotopic composition on growth rate and $[CO_2]_{aq}$: Theoretical considerations and experimental results, *Geochim. Cosmochim. Acta*, *59*, 1131-1138, 1995.

Laws, E. A., R. R. Bidigare, and B. N. Popp, Chemostat studies of the relationship between ε_p and the μ/CO_2(aq) in the marine diatom *Phaeodactylum tricornutum*: Evidence of a DIC accumulation mechanism, *Limnol. Oceanogr.*, *42*, 1552-1560, 1997.

Lynch-Stieglitz, J., T. F. Stocker, W. S. Broecker, and R. G. Fairbanks, The influence of air-sea exchange on the isotopic composition of oceanic carbon: Observations and modeling, *Global Biogeochem. Cycles*, *9*, 653-665, 1995.

Mackey, D. J., J. Parslow, H.W. Higgins, F. B. Griffiths, and J. E. O'Sullivan, Plankton production and biomass in the western equatorial Pacific: biological and physical controls, *Deep Sea Res.*, *Part II*, *42*, 499-533, 1995.

Maier-Reimer, E., Geochemical cycles in an ocean general circulation model: Preindustrial tracer distributions, *Global Biogeochem. Cycles*, *7*, 645-677, 1993.

Martin, J. H., Glacial-interglacial CO_2 change: The iron hypothesis, *Paleoceanography*, *5*, 1-13, 1990.

Martin, J. H., R. M. Gordon, and S. E. Fitzwater, Iron in Antarctic waters, *Nature*, *345*, 156-158, 1990.

Mashiotta, T. A., D. W. Lea, and H. J. Spero, Experimental determination of cadmium uptake in shells of the planktonic foraminifera *Orbulina universa* and *Globigerina bulloides*: Implications for surface water paleoreconstructions, *Geochim. Cosmochim. Acta*, *61*, 4053-4065, 1997.

Merritt, D. A., and J. M. Hayes, Factors controlling precision and accuracy in isotope-ratio-monitoring mass spectrometry, *Anal. Chem.*, *66*, 2336-2347, 1994.

Merritt, D. A., K. H. Freeman, M. P. Ricci, S. A. Studley, and J.M. Hayes, Performance and optimization of a combustion interface for isotope-ratio-monitoring gas chromatography/mass spectrometry, *Anal. Chem.*, *67*, 2461-2473, 1995.

Metzl, N., B. Tilbrook, and A. Poisson, The annual fCO_2 cycle and the air-sea CO_2 flux in the sub-Antarctic Ocean, *Tellus*, *51B*, 849-861, 1999.

Millero, F.J., The thermodynamics of the carbonic acid system in seawater, *Geochim. Cosmochim. Acta*, *43*, 1651-1661, 1979.

Millero, F. J., The thermodynamics of the carbon dioxide system in the oceans, *Geochim. Cosmochim. Acta*, *59*, 661-677, 1995.

Mook, W. G., J. C. Bommerson, and W. H. Staberman, Carbon isotope fractionation between dissolved bicarbonate and gaseous carbon dioxide, *Earth Planet. Sci. Lett.*, *22*, 169-176, 1974.

Nichols, P. D., A. C. Palmisano, G. A. Smith, and D. C. White, Lipids of the Antarctic sea-ice diatom *Nitzschia cylindrus*, *Phytochemistry*, *25*, 1649-1653, 1986.

Nichols, P. D., A. C. Palmisano, M. S. Rayner, G. A. Smith, and D. C. White, Occurrence of novel C_{30} sterols during a spring bloom, *Org. Geochem.*, *15*, 503-508. 1990.

Nichols, P. D. J. H. Skerratt, A. Davidson, H. Burton, and T. A. McMeekin, Lipids of cultured *Phaeocystis pouchetii*: Signature for food-web, biogeochemical and environmental studies in Antarctica and the Southern Ocean, *Phytochem.*, *30*, 3209-3214, 1991.

Nichols, D. S., P. D. Nichols, and C. W. Sullivan, Fatty acid, sterol, and hydrocarbon composition of Antarctic sea-ice diatom communities from McMurdo sound, *Antarc. Sci.*, *5*, 271-278, 1993.

Patterson, G. W., Sterols of algae, in *Physiology and Biochemistry of Sterols*, edited by G. W. Patterson and W. Nes, pp. 118-157, Amer. Oil Chem. Soc., Champaign, Ill., 1992.

Popp, B. N., R. Takigiku, J. M. Hayes, J. W. Louda, and E. W. Baker, The post-Paleozoic chronology and mechanism of ^{13}C depletion in primary marine organic matter, *Am. J. Sci., 289,* 436-454, 1989.

Popp, B. N., E. A. Laws, R. R. Bidigare, J. E. Dore, K. L. Hanson, and S. G. Wakeham, Effect of phytoplankton cell geometry on carbon isotopic fractionation, *Geochim. Cosmochim. Acta, 62,* 69-77, 1998.

Raven, J. A., and A. M. Johnston, Mechanisms of inorganic-carbon acquisition in marine phytoplankton and their implications for the use of other resources, *Limnol. Oceanogr., 36,* 1701-1714, 1991.

Rau, G. H., Variations in sedimentary organic $\delta^{13}C$ as a proxy for past changes in ocean and atmospheric CO_2, in *Carbon Cycling in the Glacial Ocean: Constraints on the Ocean's Role in Global Change,* edited by R. Zhan et al., NATO ASI Ser. 17, 307-321, 1994.

Rau, G. H., T. Takahashi, and D. J. Des Marais, Latitudinal variations in plankton $\delta^{13}C$: Implications for CO_2 and productivity in past oceans, *Nature, 341,* 516-518, 1989.

Rau, G. H., C. W. Sullivan, and L. I. Gordon, $\delta^{13}C$ and $\delta^{15}N$ variations in Weddell Sea particulate organic matter, *Mar. Chem., 35,* 355-369, 1991a.

Rau, G. H., T. Takahashi, D. J. Des Marais, and C. W. Sullivan, Particulate organic matter $\delta^{13}C$ variations across the Drake Passage, *J. Geophys. Res., 96,* 15131-15135, 1991b.

Rau, G. H., T. Takahashi, D. J. Des Maris, D. J. Repeta, and J. H. Martin, The relationship between $\delta^{13}C$ of organic matter and $[CO_2(aq)]$ in ocean surface water: Data from a JGOFS site in the northeast Atlantic Ocean and a model, *Geochim. Cosmochim. Acta, 56,* 1413-1419, 1992.

Rau, G.H., U. Riebesell, and D. Wolf-Gladrow, A model of photosynthetic ^{13}C fractionation by marine phytoplankton based on diffusive molecular CO_2 uptake, *Mar. Ecol. Prog. Ser., 133,* 275-285, 1996.

Rau, G.H., U. Riebesell, and D. Wolf-Gladrow, CO_{2aq}-dependent photosynthetic ^{13}C fractionation in the ocean: A model versus measurements, *Global Biogeochem. Cycles, 11,* 267-278, 1997.

Rintoul, S. R., J. R. Donguy, and D. H. Roemmich, Seasonal evolution of upper ocean thermal structure between Tasmania and Antarctica, *Deep Sea Res., Part I, 44,* 1185-1202, 1997.

Rogers, J. C., and R. B. Dunbar, Carbon isotopic composition of particulate organic carbon in Ross Sea surface waters during austral summer, *Antarc. J. U.S., 28,* 81-83, 1993.

Rosenberg, M., R. Eriksen, S. Bell, N. Bindoff, and S. Rintoul, *Aurora Australis* marine science cruise AU9407: Oceanographic field measurements and analysis, *Antarc. Coop. Res. Rep., No. 6,* 97 pp., Antarc. Div., Kingston, Tasmania, Australia, 1995.

Roy, R. N., L. N. Roy, K. M. Vogel, C. P. Moore, T. Pearson, C. E. Good, F. J. Millero, and D. M. Cambell, Determination of the ionization constants of carbonic acid in seawater, *Mar. Chem., 44,* 249-260, 1993.

Sackett, W. M., W. R. Eckelmann, M. L. Bender, and A. W. H. BÇ, Temperature dependence of carbon isotope composition in marine plankton and sediments, *Science, 148,* 235-237, 1965.

Sackett, W. M., B. J. Eadie, and M. E. Exner, Stable isotope composition of organic carbon in recent Antarctic sediments, in *Advances in Organic Geochemistry 1973,* edited by B. Tissot and F. Bienner, pp. 661-671, Pergamon, New York, 1974.

Sakshaug, E., A. Bricaud, Y. Dandonneau, P. G. Falkowski, D. A. Kiefer, L. Legendre, A. Morel, J. Parslow, and M. Takahashi, Parameters of photosynthesis: definitions, theory and interpretation of results, *J. Phytoplankton Res., 11,* 1637-1670, 1997.

Sakshaug, E., and O. Holm-Hansen, Photoadaptation in Antarctic phytoplankton: Variations in growth rate, chamical composition and P versus I curves, *J. Plankton Res., 8,* 459-473, 1986.

Sarmiento, J. L., and J. R. Toggweiler, A new model for the role of the oceans in determining atmospheric pCO_2, *Nature, 308,* 621-624, 1984.

Schouton, S., W. C. M. K. Breteler, P. Blokker, N. Schogt, W. I. C. Rijpstra, K. Grice, M. Baas, and J. S. S. Damsté, Biosynthetic effects on the stable carbon isotopic compositions of algal lipids: Implications for deciphering the carbon isotopic biomarker record, *Geochim. Cosmochim. Acta, 62,* 1397-1406, 1998.

Sedwick, P. N., and G. R. DiTullio, Regulation of algal blooms in Antarctic shelf waters by the release of iron from melting sea ice, *Geophys. Res. Lett.,* 24, 2515-2518, 1997.

Sikes, E. L., J. K. Volkman, L. G. Robertson, and J.-J. Pichon, Alkenones and alkenes in surface waters and sediments of the Southern Ocean: Implications for paleotemperature estimation in polar regions, *Geochem. Cosmochim. Acta, 61,* 1495-1505, 1997.

Six, K. D., and E. Maier-Reimer, Effects of plankton dynamics on seasonal carbon fluxes in an ocean general circulation model, *Global Biogeochem. Cycles, 10,* 559-583, 1996.

Skerratt, J. H., P. D. Nichols, T. A. McMeekin, and H. Burton, Seasonal and inter-annual changes in planktonic biomass and community structure in eastern Antarctica using signature lipids, *Mar. Chem., 51,* 93-113, 1995.

Smith, W. O., D. M. Nelson, G. R. DiTullio, and A. R. Leventer, Temporal and spatial patterns in the Ross Sea: Phytoplankton biomass, elemental composition, productivity and growth rates, *J. Geophys. Res., 101,* 18455-18465, 1996.

Strickland, J. D. H., and T. R. Parsons, *A Practical Handbook of Seawater Analysis,* 311 pp., Fisheries Res. Board Canada, 1972.

Summons, R. E., L. L. Janke, and Z. Roksandic, Carbon isotopic fractionation in lipids from methanogenic bacteria: relevance for interpretation of the geochemical record of biomarkers, *Geochem. Cosmochim. Acta, 58,* 2853-2863, 1994.

Volkman, J. K., A review of sterol markers for marine and terrigenous organic matter, *Org. Geochem., 9,* 83-99, 1986.

Volkman, J. K., G. Eglinton, E. D. S. Corner, and J. R. Sargent, Novel unsaturated straight-chained methyl and ethyl ketones in marine sediment and a coccolithophorid *Emiliania huxleyi,* in *Advances in Organic Geochemistry, 1979,* edited by A. C. Douglas and J. R. Maxwell, pp. 219-227, Pergamon Press, New York, 1981.

Volkman, J. K., S. M. Barrett, G. A. Dunstan, and S. W. Jeffrey, Geochemical significance of the occurrence of dinosterol and other 4-methyl sterols in a marine diatom, *Org. Geochem., 20,* 7-16, 1993.

Voogt, P. A., Composition and biosynthesis of sterols in some sponges, *Neth. J. Zool., 26,* 84-93, 1976.

Wada, E., M. Terazaki, Y. Kabaya, and T. Nemoto, ^{15}N and ^{13}C abundances in the Antarctic Ocean with emphasis on the biogeochemical structure of the food web, *Deep Sea Res., Part A, 34,* 829-841, 1987.

Wakeham, S. G., and E. A. Canuel, Organic geochemistry of particulate organic matter in the eastern tropical North Pacific Ocean: Implications for particle dynamics, *J. Mar. Res., 46,* 183-213, 1988.

Wedeking, K. W., J. M. Hayes, and U. Matzigkeit, Procedure of organic geochemical analysis, in *Earth's Earliest Biosphere: Its Origin and Evolution,* edited by J. W. Schopf, pp. 428-441, Princeton Univ. Press, Princeton, N.J., 1983.

Weiss, R.F., Carbon dioxide in water and seawater: The solubility of a non-ideal gas, *Mar. Chem., 2,* 203-214, 1974.

Wong, A., N. L. Bindoff, and A. Forbes, Ocean ice-shelf interaction and possible bottom water formation in Prydz Bay, Antarctica, *Antarc. Res. Ser.,* AGU, Washington, D.C., in press, 1998.

Worby, A. P., R. A. Massom, I. Allison, V. I. Lytle, and P. Heil, East Antarctic sea ice: A review of its structure, properties and drift, in *Antarctic Sea Ice: Physical Processes, Interactions and Variability, Antarc. Res. Ser.,* vol. 74, edited by M. Jeffries, pp. 41-67, AGU, Washington, D.C., 1998.

Wright, S. W., and S. W. Jeffrey, High resolution HPLC system for chlorophylls and carotenoids of marine phytoplankton, in *Phytoplankton Pigments in Oceanography: Guidelines to Modern Methods,* edited by S. W. Jeffrey, et al., pp. 327-341, United Nat. Educ., Sci., and Cult. Org., Paris, 1997.

R. R. Bidigare, E. A. Laws, B. N. Popp, and T. M. Rust, School of Ocean and Earth Science and Technology, University of Hawaii, 2525 Correa Road, Honolulu, HI 96822. (popp@soest.hawaii.edu)

F. B. Griffiths, B. Tillbrook, and T. Trull, Antarctic CRC, University of Tasma , Hobart, Tasmania, 7000 Australia.

F. Kem Department of Geological Sciences, University of Illinois at Chicago, Cl ago, IL 60607.

H. J. Mar ..ant and S. W. Wright, Australian Antarctic Division, Kingston, Tasmania, 7050 Australia.

S. G. Wakeham, Skidaway Institute of Oceanography, Savannah, GA 31411.